Modal Modeling and Structural Dynamics Modification

David Formenti
Sound and Vibration Engineer
BlackHawk Technology
Santa Cruz, CA 95060
formenti@blkhawk.com

Mark Richardson
President & CEO
Vibrant Technology, Inc.
Centennial, CO 80112

Structural Dynamics Modification (SDM) also known as eigenvalue modification [1], has become a practical tool for improving the engineering designs of mechanical systems. It provides a quick and inexpensive approach to investigating the effects of design modifications on the resonances of a structure, thus minimizing the need for costly prototype fabrication and testing.

Modal Models

SDM is unique in that it works directly with a modal model of the structure, either an **Experimental Modal Analysis (EMA)** modal model, a **Finite Element Analysis (FEA)** modal model, or a **Hybrid** modal model consisting of both EMA and FEA modal parameters. EMA mode shapes are obtained from experimental data and FEA mode shapes are obtained from an analytical finite element computer model.

A **modal model** consists of a set of ***scaled mode shapes***. In this Tech Paper the mode shapes used in a modal model are scaled to **Unit Modal Masses**, called **UMM mode shapes**. FEA mode shapes are commonly scaled to **UMM mode shapes** using the mass matrix of the FEA model. In this Tech Paper , it will be shown how EMA mode shapes can also be scaled to **UMM mode shapes** without using a mass matrix.

A modal model preserves the mass, damping, and stiffness properties of a mechanical structure, and is used by SDM to represent the dynamic properties of the unmodified structure.

Design Modifications

Once the dynamic properties of an unmodified structure are defined in the form of its modal model, SDM can be used to predict the dynamic effects of mechanical design modifications to the structure. These modifications can be as simple as ***additions to*** or ***removals of*** point masses, linear springs, or linear dampers, or more complex modifications can be modeled using FEA elements such as rod and beam elements, plate elements (membranes) and solid elements such as prisms, tetrahedrons, and brick elements.

SDM is computationally very efficient because it solves an eigenvalue problem in ***modal space***. In contrast, FEA mode shapes are obtained by solving an eigenvalue problem in ***physical space***.

Another advantage of SDM is that the modal model of the unmodified structure must only contain data for the DOFs (points & directions) ***where the modification elements are attached*** to a geometric model of the structure. SDM then provides a new modal model of the modified structure, as depicted in Figure 1.

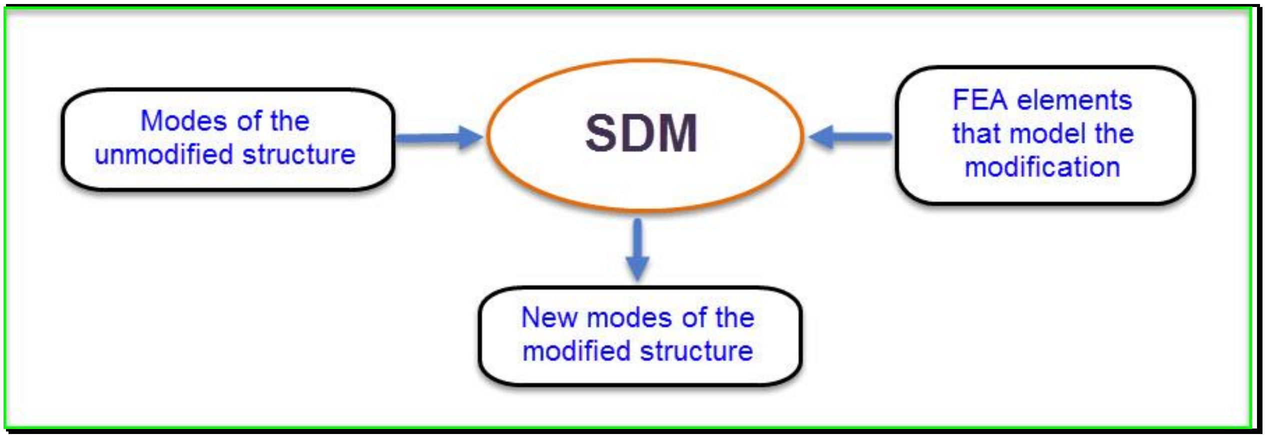

Figure 1. SDM Input-Output Diagram

Eigenvalue Modification

A variety of numerical methods have been developed over the years which only require a modal model to represent the dynamics of an unmodified structure. Among the more traditional methods for performing these calculations are ***modal synthesis***, the ***Lagrange multiplier*** method, and ***diakoptics*****.** However, the ***local eigenvalue modification*** technique, developed primarily through the work of Weissenburger, Pomazal, Hallquist, and Snyder [1], is the technique commonly used by the SDM method today.

All of the early development work on SDM was done primarily with analytical FEA mode shapes. The primary objective was to provide a faster means of investigating physical changes to a structure without having to solve a much larger eigenvalue problem. FEA mode shapes are obtained by solving the problem in physical coordinates, whereas SDM solves a much smaller eigenvalue problem in modal coordinates.

In 1979, Structural Measurement Systems (SMS) began using the local eigenvalue modification method together with an EMA modal model derived from a modal test. [2]-[5]. The computational efficiency of this method made it very attractive for use in a laboratory on a desktop calculator or computer. More importantly, it gave reasonably accurate results using only a small number of EMA mode shapes in the modal model of the unmodified structure.

A modal model with only a few mode shapes in it is called a ***truncated modal model***. Regardless of whether EMA or FEA mode shapes are used, ***truncated modal model***s have been shown to adequately characterize the dynamics of a structure. The effects of using truncated modal models was investigated in [2] and [3].

The fundamental calculation of SDM is the solution of an eigenvalue problem. The solution is computationally efficient because a small dimensional eigenvalue problem is solved. Computational speed is virtually independent of the number of DOFs in the modal model. Hence, large modifications involving many DOFs are handled as efficiently as smaller modifications.

The SDM computational process is straightforward. All physical modifications are converted into appropriate changes to the mass, stiffness, & damping matrices of the equations of motion, in the same manner as an FEA model is constructed. These modification matrices are then transformed to modal coordinates using the mode shapes of the modal model of the unmodified structure. The resulting transformed modifications are then added to the modal properties of the unmodified structure, and these new equations are solved for the new modes of the modified structure.

To illustrate this process, if there were 1000 DOFs in an FEA model, solving for its FEA mode shapes requires the solution of an eigenvalue problem with mass & stiffness matrices of the size (1000 by 1000). By contrast, if the dynamics of an unmodified structure is represented with a modal model consisting of ten mode shapes, new mode shapes resulting from a structural modification are found by solving an eigenvalue problem with transformed mass & stiffness matrices of the size (10 by 10).

The size of the eigenvalue problem in modal space is independent of the number of structural modifications made to the structure. Many modification elements can be attached to a 3D geometric model of the structure, and the SDM solution time does not significantly increase.

SDM requires two inputs,

1. A modal model that adequately represents the dynamics of the unmodified structure
2. Finite elements attached to a geometric model of the structure that characterize the structural modifications

With these inputs, SDM calculates a new modal model that represents the dynamics of the modified structure. It will also be shown in later examples that SDM obtains results that are very comparable to those obtained from an FEA eigen-solution.

Measurement Chain to Obtain an EMA Modal Model

If a modal model containing EMA mode shapes is used with SDM, the accuracy of the mode shapes will directly influence the accuracy of the results calculated with the SDM method. To understand the potential errors that can occur in an EMA modal model, in is important to review the steps in the ***measurement chain*** required to obtain EMA mode shapes.

Three major steps are commonly used to obtain an EMA modal model

1. Acquire experimental vibration data from the test article
2. Calculate a set of Frequency Response Functions (FRFs) from the vibration data
3. Curve fit the FRFs to estimate the EMA mode shapes of the test article

Critical Issues in the Measurement Chain

Following is a list of issues to consider in implementing a measurement chain,

1. Non-linearity of the test structure dynamics
2. Boundary conditions of the test structure
3. Excitation technique
4. Force and response sensors
5. Sensor mounting
6. Sensor calibration
7. Sensor cabling

8. Signal acquisition and conditioning
9. Spectrum analysis
10. FRF calculation
11. FRF curve fitting
12. Creating an EMA modal model

All of these issues involve assumptions that can impact the accuracy of the EMA modal model and ultimately the accuracy of the SDM results. Only a few of these critical issues will be addressed here, namely; sensors, sensor mounting, sensor calibration, FRF calculation, and FRF curve fitting.

Calculating FRFs from Experimental Vibration Data

To create an EMA modal model, a set of calibrated inertial FRF measurements is required. These frequency domain measurements are unique in that they involve subjecting the test structure to a known measurable force while simultaneously measuring the structural response(s) due to the force. The structural response is measured either as acceleration, velocity, or displacement using sensors that are either mounted on the surface or are non-contacting but still measure the surface vibration.

An FRF is a special case of a Transfer Function. A Transfer Function is a frequency domain relationship between any type of input signal and any type of output signal. An FRF defines the dynamic relationship between the excitation force applied to a structure at a specific location in a specific direction and the resulting response motion at another specific location in a specific direction. The force input point & direction and the response point & direction are referred to as the Degrees of Freedom (or DOFs) of the FRF.

An FRF is also called a ***cross-channel measurement***. It requires the ***simultaneous acquisition*** of both the excitation force and one of its resultant responses. This means that at least a 2-channel data acquisition system or spectrum analyzer is required to measure the signals required to calculate an FRF. The force (input) and the response (output) signals must also be ***simultaneously acquired***, meaning that both channels of data are amplified, filtered, and sampled without introducing any artificial phase difference between the two signals.

Sensing Force & Motion

The excitation force is typically measured with a load cell. The analog signal from the load cell is fed into one of the channels of the data acquisition system. The response is measured either with an accelerometer, laser vibrometer, displacement probe, or another sensor that can measure the surface vibration. Accelerometers are most often used today because of their availability, relatively low cost, and variety of sizes and sensitivities. The important characteristics of both the load cell and accelerometer are:

1. Sensitivity
2. Usable amplitude range
3. Usable frequency range
4. Transverse sensitivity
5. Mounting method

Sensitivity Flatness

The most common type of sensor today is referred to as an IEPE/CCLD/ICP/Deltatron/Isotron style of sensor. This type of sensor requires a 2-10 milli-amp current supply, typically supplied by the data acquisition system, and has a built-in charge amplifier and other signal conditioning. It also has a fixed sensitivity. Typical sensitivities are 10mv/lb or 100mv/g.

The ideal frequency spectrum for any sensor is a ***"flat magnitude"*** over its usable frequency range. The documented sensitivity of most sensors is typically given at a fixed frequency (such as 100Hz, 159.2Hz, or 250Hz), and is referred to as its 0-dB level.

The sensitivity of an accelerometer is specified in units of mv/g or mv/(m/s^2) with a ***typical accuracy of +/-5%*** at a specific frequency. The frequency spectrum of all sensors in ***not perfectly flat***, meaning that its sensitivity varies somewhat over its useable frequency range. The response amplitude of an ICP accelerometer typically ***rolls off*** at low frequencies and ***rises*** at the high end of its useable frequency range. This specification is the ***flatness*** of the sensor, with a ***typical variance of +/-10% to +/-15%***.

All of this equates to a possible error in the sensitivity of the force or response sensor over its usable frequency range. This means that the amplitude of an FRF might be in error by the amount that the sensitivity changes over its measured frequency range.

Transverse Sensitivity

Adding to its flatness error is the ***transverse sensitivity*** of a sensor. Both force and vibration have a direction associated with them. That is, a force or motion is defined at a point in a specific direction.

A uniaxial (single axis) transducer should only output a signal due to force or motion in the direction of its sensitive axis. Ideally, any force or motion that is not along its sensitive axis should not yield an output signal, but this is not the case with most sensors.

All sensors have a documented specification called ***transverse sensitivity*** or ***cross axis sensitivity***. Transverse sensitivity specifies how much of the sensor output is due to a force or motion that is sensed from a direction ***other than the measurement axis*** of the sensor. Transverse sensitivity is typically ***less than 5%*** of the sensitivity of the measurement axis. For example, if an accelerometer has a sensitivity of 100mv/g, its transverse sensitivity might be 5%, or about 5mv/g. Therefore, 1g of motion in a direction other than the sensitive axis of an accelerometer might add 5mv (or 0.05g) to its output signal.

Sensor Linearity

Another area affecting the accuracy of an FRF is the ***linearity*** of each sensor output signal relative to the actual force or vibration. If a sensor output signal were plotted as a function of its input force or vibration, all its output values should ***lie on a straight line***. Any values that do not lie on a straight line are an indication of the ***non-linearity*** of the sensor. The ***non-linearity*** specification is ***typically less than 1%*** over the useable frequency range of a sensor.

As the amplitude of the measured signal becomes larger than the specified input amplitude range of the sensor, the signal will ultimately ***cause an overload*** in the internal amplifier of the sensor.

This overload results in a ***clipped output signal*** from the sensor. A ***clipped output signal*** is the reason why it is very important to measure amplitudes that are within the specified amplitude range of a sensor.

Sensor Mounting

Attaching a sensor to the surface of the test article is also of critical importance. The function of a sensor is to ***"transduce"*** a physical quantity, for example the acceleration of the surface at a point in a direction. Therefore, it is important to attach the sensor to a surface so that it will accurately transduce the surface motion over the frequency range of interest.

Mounting materials and techniques also have a useable frequency range just like the sensor itself. It is very important to choose an appropriate mounting technique so that the surface motion over the desired frequency range is not affected by the mounting material of method. The use of ***magnets, tape, putty***, **glue**, or ***contact cement*** are all convenient for attaching sensors to surfaces. But attaching a sensor using a ***threaded stud*** is the most reliable method, with the widest frequency range.

Leakage Error

Another error associated with the FRF calculation is a result of the FFT algorithm itself. The FFT algorithm is used to calculate the Digital Fourier Transform (DFT) of the force and response signals. These DFT's are then used to calculate an FRF.

Finite Length Sampling Window

The FFT algorithm assumes that the time domain window of acquired digital data (called the ***sampling window***) ***completely contains*** the acquired signal. If an acquired signal is not fully captured within its sampling window, the DFT of the signal will contain ***leakage error***.

Leakage-Free Spectrum

The spectrum of an acquired signal will be ***leakage-free*** if one of the following conditions is satisfied.

1. If a signal is ***periodic*** (like a ***sine wave***), then it must make ***one or more complete cycles*** within the sampled window
2. If a signal is ***not periodic***, then it must be ***completely contained*** within the sampled window

If an acquired signal does not meet one of the above conditions, there will be errors in its DFT, and errors in the FRF that is calculated using the DFT. Leakage error causes both amplitude and frequency errors in a DFT and in a FRF that uses the DFT.

Leakage-Free Signals

Leakage is eliminated by using testing signals that meet one of the two conditions stated above. During Impact testing, if the impulsive force and the impulse response signals are both completely contained within their sampling windows, ***leakage-free FRFs*** will be calculated using those signals.

During shaker testing, if a Burst Random or a Burst Chirp (fast swept sine) shaker signal is used to excite the structure, ***leakage-free FRFs*** can be calculated using those signals. A Burst Random or Burst Chirp signal is terminated prior to the end of its sampling window so that both the force and structural response signals are ***completely contained*** within their sampling windows.

Reduced Leakage

If one of the two leakage-free conditions cannot be met by the acquired force and response signals, then leakage errors ***can be minimized*** in their spectra by applying an appropriate time domain window to the sampled signal before it is transformed using the FFT. A ***Hanning window*** is typically applied to pure (continuous) random signals. Pure random signals are ***never completely contained*** within their sampling windows. Using a Hanning window prior to transforming them with the FFT will minimize leakage in their frequency spectrum.

Linear versus Non-Linear Dynamics

Both EMA and FEA modal models are defined as solutions to a set of ***linear differential equations.*** Using a modal model assumes that ***the linear dynamic behavior*** of the test article can be ***adequately described using these equations***. However, many real-world structures may not exhibit linear dynamic motion.

Real-world structures can have dynamic behavior ranging from ***linear*** to ***slightly non-linear*** to ***severely non-linear***. If the test article is in fact undergoing non-linear motion, significant errors will occur when attempting to extract modal parameters from a set of FRFs which are based on a linear dynamic model.

Random Excitation & Spectrum Averaging

To reduce the effects of non-linear behavior, random excitation combined with signal post-processing must be applied to the acquired data. The goal is to yield a set of ***linear FRF estimates*** to represent the dynamics of the structure subject to a certain force level.

This common method for testing a non-linear structure is to excite it with one or more shakers using random excitation signals. If these signals continually vary over time, the random excitation will excite the non-linear behavior of the structure in a random fashion.

Each time a non-linear signal is transformed using the FFT, the non-linear components of the signal will appear as ***random noise*** spread over the frequency range of the DFT. If multiple DFTs of the response of a randomly excited structure are ***averaged together***, the non-linear components (random noise) will be ***"averaged out"*** of the average DFT, leaving only the ***linear resonant response peaks***.

Curve Fitting FRFs

The first step of an ***FRF-based EMA*** is to calculate a set of FRFs that accurately represent the linear dynamics of the test article over a frequency range of interest. The second step is to curve fit the FRFs using a ***linear parametric model*** of an FRF. The unknown parameters of the FRF model are the modal parameters of the structure. The goal of these two steps is to obtain an ***accurate EMA modal model***.

If the test article has a high modal density including either ***closely coupled modes*** (two modes represented by one resonance peak) or ***repeated roots*** (two modes with the same frequency but different mode shapes), extracting an accurate EMA modal model from the FRFs can be challenging.

The linear parametric curve fitting model is a ***summation of contributions from all modes*** at each frequency sample of the FRFs. This model is commonly curve fit to the FRF data using a ***least-squared-error*** method. This broadband curve fitting approach also assumes that all resonances of interest have been adequately excited over the frequency span of the FRFs.

A wide variety of FRF-based curve fitting methods are commercially available today. All FRF-based curve fitting methods assume that the FRFs adequately represent the linear dynamics of the test article and are leakage-free.

Modal Models and SDM

SDM will give accurate results when an accurate modal model of the unmodified structure is used. The modal model can contain EMA mode shapes, FEA mode shapes, Hybrid mode shapes consisting of both EMA and FEA modal parameters, or a mixture of all three types of mode shapes.

The advantage of SDM is that with a reasonably accurate modal model of the unmodified structure, numerous structural modifications can be quickly explored. This could include exploring alternate boundary conditions which are difficult to model with an FEA model.

Later in this Tech Paper , a Hybrid modal model containing both translational & rotational DOFs will be used with SDM to model the attachment of a RIB stiffener to an aluminum plate. The new mode shapes calculated by SDM will then be compared with both FEA & EMA mode shapes of the plate with the RIB attached to it.

Structural Dynamic Models

The dynamic behavior of a mechanical structure can be modeled either with a set of differential equations in the time domain, or with an equivalent set of algebraic equations in the frequency domain. Once the equations of motion have been created, they can be used to calculate mode shapes and to calculate structural responses to static loads or dynamic forces.

The dynamic response of most structures usually includes ***resonance-assisted vibration.*** Dynamic resonance-assisted response levels can ***far exceed*** the deformation levels due to static loads. Resonance-assisted vibration is often the cause of noisy operation, uncontrollable behavior, premature wear out of parts such as bearings, and unexpected material failure due to cyclic fatigue.

Structural Resonances

Two or more spatial deformations assembled into a vector format is called an Operating Deflection Shape (or ODS).

A mode of vibration is a mathematical representation of a structural resonance. An ODS is a ***summation of mode shapes***.

Each mode is represented by its natural frequency (its modal frequency), a damping decay constant (the decay rate of a resonance when forces are removed from the structure), and its spatially distributed amplitude levels (its mode shape). These three modal properties (frequency, damping, and mode shape) provide a ***complete mathematical representation*** of each structural resonance. A mode shape is the contribution of a resonance to the overall deformation (the ODS) on the surface of a structure at each location in each direction.

It is shown later that both the time and frequency domain equations of motion can be represented solely in terms of modal parameters. This powerful conclusion means that a set of modal parameters can be used to ***completely represent the linear dynamics*** of a structure.

When properly scaled, a set of mode shapes is called a ***modal model***. The complete dynamic properties of the structure are represented by its modal model. SDM uses the ***modal model*** of the ***unmodified*** structure together with the FEA elements that represent structural modifications as inputs and calculates a ***new modal model*** for the modified structure.

Truncated Modal Model

All EMA and FEA modal models contain mode shapes for a ***finite number of modes***. An EMA modal model contains a finite number of mode shapes that were obtained by curve fitting a set of FRFs that span a ***limited frequency range***. An FEA modal model also contains a finite number of mode shapes that are defined for a ***limited range of frequencies***. Therefore, both EMA and FEA modal models represent a ***truncated (approximate) dynamic model*** of a structure.

Except for so-called lumped parameter systems, (like a mass on a spring), all real-world structures have an ***infinite number of resonances***. But SDM still provides usable results because of the following property.

The dynamic response of most structures ***is dominated*** by the excitation of their ***low frequency modes***.

When using the SDM method, ***all the low frequency modes*** should be included in the modal model. In order to account for the higher frequency modes that have been left out of the truncated modal model, it is also important to include several modes ***above the highest frequency mode*** of interest in the modal model.

Sub structuring

To solve a sub structuring problem, where one structure is mounted on or attached to another using FEA elements, the free-body dynamics (the ***six rigid-body modes***) of the structure to be mounted on the other must also be included in its modal model. This will be illustrated by the example later in this Tech Paper

Rotational DOFs

Another potential source of error in using SDM is that certain modifications require mode shapes with both translational and rotational DOFs. Normally only translational motions are acquired experimentally, and therefore the resulting FRFs and mode shapes only have translational DOFs. If a modal model does not contain rotational DOFs, accurate modifications that involve torsional stiffnesses and/or rotary inertia effects cannot be accurately modeled.

FEA mode shapes derived from ***rod, beam, and plate (membrane) elements*** have rotational DOFs included in them. When rotational stiffness and inertia are important, FEA mode shapes with rotational DOFs in them can be used in a Hybrid modal model as input to SDM. Later in this Tech Paper , SDM will be used to model the attachment of a RIB stiffener to a plate structure. Mode shapes with rotational DOFs and spring elements with rotational stiffness will be used to correctly model the joint stiffness between the RIB and the plate.

Time Domain Dynamic Model

Modes of vibration are defined by assuming that the dynamic behavior of a mechanical structure or system ***can be adequately described*** by a set of time domain differential equations. These equations are a statement of ***Newton's second law*** **(F = Ma)**. They represent a ***force balance*** between the internal inertial (mass), dissipative (damping), and restoring (stiffness) forces, and the external forces acting on the structure. This force balance is written as a set of linear differential equations,

$$[\mathbf{M}]\{\ddot{\mathbf{x}}(\mathbf{t})\}+[\mathbf{C}]\{\dot{\mathbf{x}}(\mathbf{t})\}+[\mathbf{K}]\{\mathbf{x}(\mathbf{t})\} = \{\mathbf{f}(\mathbf{t})\} \qquad (1)$$

where

$[\mathbf{M}]$ 🡐 Mass matrix (**n** by **n**)
$[\mathbf{C}]$ 🡐 Damping matrix (**n** by **n**)
$[\mathbf{K}]$ 🡐 Stiffness matrix (**n** by **n**)
$\{\ddot{\mathbf{x}}(\mathbf{t})\}$ 🡐 Accelerations (**n**-vector)
$\{\dot{\mathbf{x}}(\mathbf{t})\}$ 🡐 Velocities (**n**-vector)
$\{\mathbf{x}(\mathbf{t})\}$ 🡐 Displacements (**n**-vector)
$\{\mathbf{f}(\mathbf{t})\}$ 🡐 Externally applied forces (**n**-vector)

These differential equations describe the ***dynamics between n-discrete points & directions*** or ***n-degrees-of-freedom (DOFs)*** of a structure. To adequately describe its dynamic behavior, enough equations can be created involving as many DOFs as necessary. Even though equations could be created between an infinite number of DOFs, in a practical sense only a finite number of DOFs is ever used, but they could still number in the 100's of thousands.

Notice that the damping force is ***proportional to velocity***. This is a model for ***viscous damping***. Different damping models are addressed later in this Tech Paper .

Finite Element Analysis (FEA)

Finite element analysis (FEA) is used to generate the coefficient matrices of the time domain differential equations written above. The mass and stiffness matrices are generated from the physical and material properties of the structure. Material properties include the ***modulus of elasticity***, ***inertia***, and ***Poisson's ratio*** (or ***"sqeezability"***).

Damping properties are not easily modeled for real-world structures. Hence the damping force term is usually left out of an FEA model. Even without damping, the mass and stiffness terms are enough to model resonant vibration, hence the equations of motion can be solved for modal parameters.

FEA Modes

The ***homogeneous*** form of the differential equations, where the external forces on the right-hand side are zero, can be solved for mode shapes and their corresponding natural frequencies. This is called an ***eigen-solution***. Each natural frequency is an ***eigenvalue***, and each mode shape is an ***eigenvector.*** The analytical mode shapes are referred to as **FEA mode shapes**. The transformation of the equations of motion (1) into modal coordinates is covered later in this Tech Paper

Frequency Domain Dynamic Model

In the frequency domain, the dynamics of a mechanical structure or system are represented by a set of linear algebraic equations, in a form called a ***Transfer Function*** model or ***MIMO (Multiple Input Multiple Output) model***. This model contains Transfer Functions between all combinations of ***input and response DOF pairs***,

$$\{\mathbf{X(s)}\} = [\mathbf{H(s)}]\{\mathbf{F(s)}\} \qquad (\mathbf{n}\text{-vector}) \tag{2}$$

where

$\mathbf{s}$ ← Laplace variable (complex frequency)
$[\mathbf{H}(\mathbf{s})]$ ← Transfer Function matrix (**n** by **n**)
$\{\mathbf{X}(\mathbf{s})\}$ ← Laplace transform of displacements (**n**-vector)
$\{\mathbf{F}(\mathbf{s})\}$ ← Laplace transform of externally applied forces (**n**-vector)

This model is also a complete description of the ***dynamics between n-DOFs*** of a structure. Equations can be created between as many DOF pairs of the structure as necessary to adequately describe its dynamic behavior over a frequency range of interest. Like the time domain differential equations (1), these equations (2) are finite dimensional.

Parametric Models Used for Curve Fitting

Curve fitting is a numerical process by which an analytical FRF model is matched to experimental FRF data in a manner that ***minimizes the squared error*** between the experimental data and the analytical curve fitting model. The purpose of curve fitting is to estimate the unknown modal parameters of the curve fitting model. More precisely, the modal frequency, damping, and mode shape of each resonance in the frequency range of the FRFs is estimated by curve fitting an analytical model to a set of FRFs.

Rational Fraction Polynomial Model

The Transfer Function matrix in equation (2) can also be expressed analytically as a ratio of two polynomials. This is called a ***rational fraction polynomial matrix form*** of the Transfer Function matrix. Expressed in terms of **m**-modes, the denominator polynomial has (**2m +1**) terms and each numerator polynomial has (**2m** terms).

$$[\mathbf{H(s)}] = \frac{[\mathbf{b_0}]\mathbf{s^{2m-1}} + [\mathbf{b_1}]\mathbf{s^{2m-2}} + [\mathbf{b_2}]\mathbf{s^{2m-3}} + \ldots + [\mathbf{b_{2m-1}}]}{\mathbf{a_0 s^{2m}} + \mathbf{a_1 s^{2m-1}} + \mathbf{a_2 s^{2m-2}} + \ldots + \mathbf{a_{2m}}} \qquad (\mathbf{n} \text{ by } \mathbf{n}) \tag{3}$$

where

$\mathbf{m} =$ Number of modes in the analytical curve fitting model

$\mathbf{a_0 s^{2m} + a_1 s^{2m-1} + a_2 s^{2m-2} + \ldots + a_{2m}}$ ← the characteristic polynomial

$\mathbf{a_0, a_1, a_2, \ldots, a_{2m}}$ ← real valued coefficients

$\mathbf{[b_0]s^{2m\text{-}1} + [b_1]s^{2m\text{-}2} + [b_2]s^{2m\text{-}3} + \ldots + [b_{2m\text{-}1}]}$ ← numerator polynomial matrix (**n** by **n**)

$\mathbf{[b_0],[b_1],[b_2], \ldots, [b_{2m\text{-}1}]}$ ← real valued coefficient matrices (**n** by **n**)

Each Transfer Function in the (**n** by **n**) matrix has a ***unique numerator polynomial*** (**n** by **n**) matrix and the ***same denominator polynomial***, called the ***characteristic polynomial***.

Partial Fraction Expansion Model

The Transfer Function matrix in equation (2) can also be expressed in ***partial fraction expansion form***. When expressed as shown in equations (4) & (5) below, any Transfer Function value ***at any frequency*** is a ***summation of terms***, each term ***called the resonance curve of a mode of vibration***.

$$\mathbf{[H(s)]} = \sum_{\mathbf{k=1}}^{\mathbf{m}} \frac{\mathbf{[r_k]}}{\mathbf{2j\,(s-p_k)}} - \frac{\mathbf{[r_k^*]}}{\mathbf{2j\,(s-p_k^*)}} \qquad (4)$$

or,

$$\mathbf{[H(s)]} = \sum_{\mathbf{k=1}}^{\mathbf{m}} \frac{\mathbf{A_k\{u_k\}\{u_k\}^t}}{\mathbf{2j\,(s-p_k)}} - \frac{\mathbf{A_k^*\{u_k^*\}\{u_k^*\}^t}}{\mathbf{2j\,(s-p_k^*)}} \qquad (5)$$

where,

$\mathbf{m} =$ number of modes of vibration
$[\mathbf{r_k}]$ ← Residue matrix for the k^{th} mode (**n** by **n**)
$\mathbf{p_k = -\sigma_k + j\omega_k}$ ← Pole location for the k^{th} mode
$\boldsymbol{\sigma_k}$ ← Damping decay of the k^{th} mode
$\boldsymbol{\omega_k}$ ← Damped natural frequency of the k^{th} mode
$\{\boldsymbol{u_k}\}$ ← Mode shape for the k^{th} mode (**n**-vector)
$\mathbf{A_k}$ ← Scaling constant for the k^{th} mode
t – denotes the transposed vector

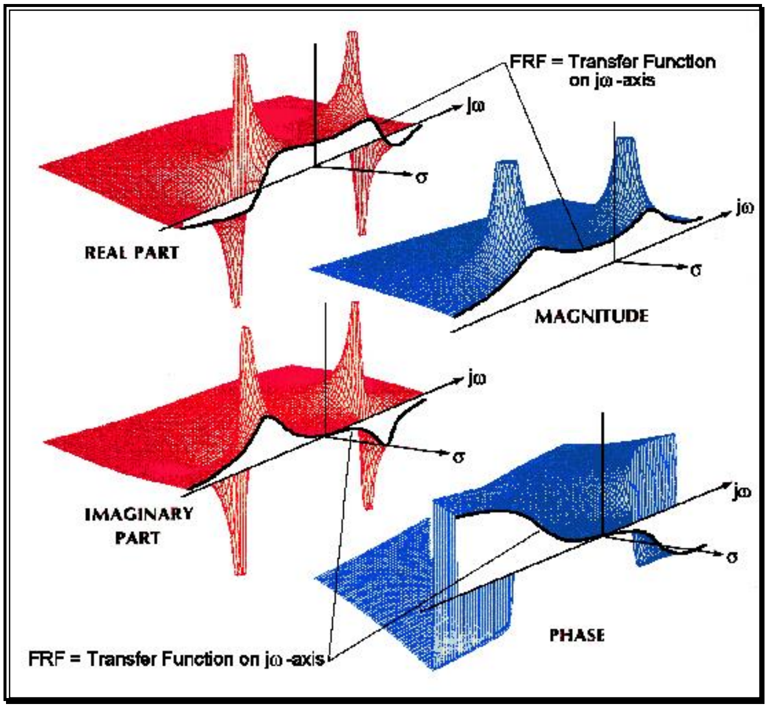

Figure 2. Transfer Function & FRF of a Single Resonance

Figure 2 shows a Transfer Function for a single resonance, plotted over ***half of the s-plane***.

Experimental FRFs

An FRF is defined as the ***values of a Transfer Function along the jω-axis*** in the s-plane

An experimental FRF can be calculated from acquired experimental data if ***each excitation force*** and ***all responses caused by that force*** are ***simultaneously acquired***. Figure 3 shows the magnitude & phase of a typical experimental FRF.

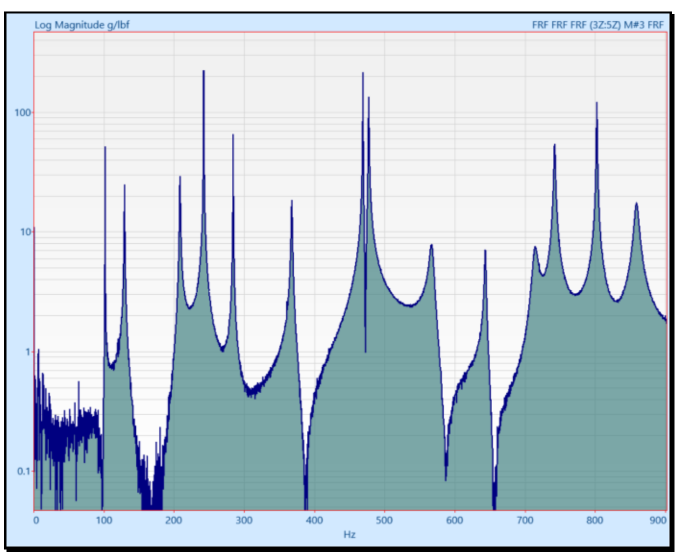

Figure 3. Log Magnitude of an Experimental FRF

FRF-Based Curve Fitting

Curve fitting is commonly done using a ***least-squared error algorithm*** which minimizes the difference between an analytical FRF model and the experimental data. The outcome of ***FRF-based curve fitting*** is a pole estimate (frequency & damping) and a mode shape (a ***row or column of residue estimates*** in the residue matrix) for each resonance that is represented in the experimental FRF data.

All forms of the curve fitting model, equations (3), (4) & (5), are used by different curve fitting algorithms. If the rational fraction polynomial model (3) is used, its numerator and denominator polynomial coefficients are determined during curve fitting. These polynomial coefficients are further processed numerically to extract the frequency, damping, & mode shape of each resonance represented in the FRFs.

Modal Frequency & Damping

Modal frequency & damping are calculated as the ***roots of the characteristic polynomial***. The denominators of all three curve fitting models (3), (4), & (5) contain the same characteristic polynomial. Therefore, ***global estimates*** of modal frequency & damping are normally obtained by curve fitting an entire set of FRFs.

Another property resulting from the common denominator of the FRFs is that the ***resonance peak for each*** mode will occur at the ***same frequency*** in each FRF. Mass loading effects can occur when the response sensors add a significant amount of mass relative to the mass of the test structure. If the sensors are moved from one point to another during a test, some resonance peaks will occur at a different frequency in certain FRFs. When mass loading of this type occurs, a ***local polynomial curve fitter***, which estimates frequency, damping & residue for each mode in each FRF, will provide better results.

Modal Residue

The modal residue, or FRF numerator, ***is unique for each mode and each FRF***.

A modal residue is the ***magnitude (or strength)*** of a mode in an FRF. A ***row or column*** of residues in the residue matrix ***defines the mode shape*** of a mode.

The relationship between residues and mode shapes is shown in the numerators of the two curve fitting models (4) & (5).

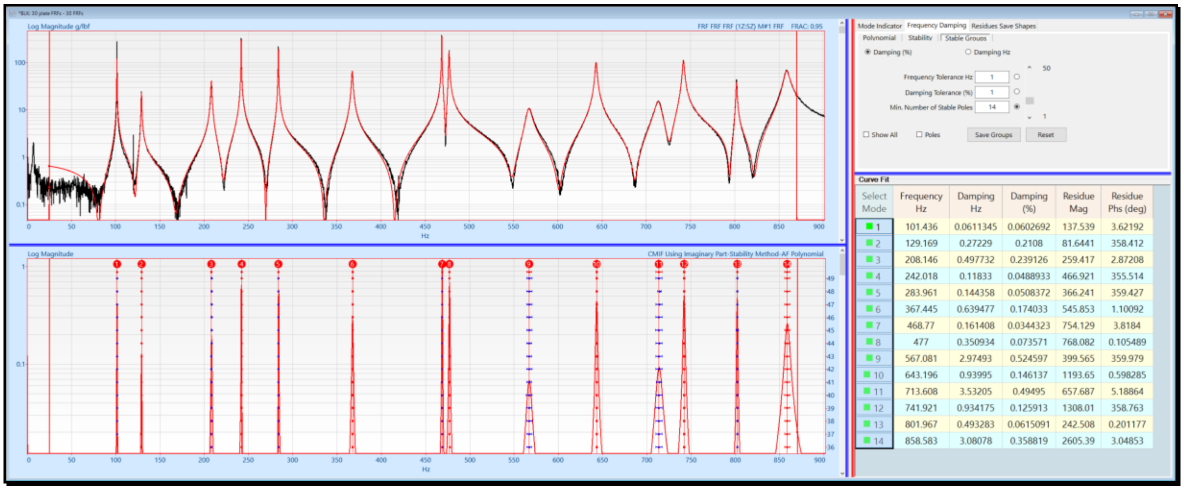

Figure 4. Curve of an Experimental FRF

Figure 4 shows an analytical curve fitting function overlaid on the log magnitude of an experimental FRF.

If the partial fraction expansion model (5) is used, the pole (frequency & damping) and residues for each mode are explicitly determined during the curve fitting process. To achieve more numerical stability, curve fitting can be divided into two curve fitting steps.

1. Estimate frequency & damping (global or local estimates)
2. Estimate residues using the frequency & damping estimates

Transformed Equations of Motion

Since the differential equations of motion (1) are linear, they can be transformed to the frequency domain using the Laplace transform without loss of any information. In the Laplace (complex frequency) domain, the equations have the form:

$$\mathbf{s^2[M]\{X(s)\}+s[C]\{X(s)\}+[K]\{X(s)\} = \{F(s)\} + \{ICs\}} \qquad (7)$$

where

$\{\mathbf{ICs}\}$ ← vector of initial conditions (**n**-vector)

$\{\mathbf{X(s)}\}$ ← Laplace transforms of displacements (**n**-vector)

$\{\mathbf{F(s)}\}$ ← Laplace transforms of applied forces (**n**-vector)

All physical properties of the structure are preserved in the left-hand side of the equations, while the applied forces and initial conditions {ICs} are contained on the right-hand side. The initial conditions can be treated as a special form of the applied forces, and hence will be dropped from consideration without loss of generality in the following development.

The equations of motion can be further simplified,

$$\mathbf{[B(s)]\{X(s)\} = \{F(s)\}} \qquad (\mathbf{n}\text{-vector}) \qquad (8)$$

where

$$[\mathbf{B}(\mathbf{s})] = \mathbf{s}^2[\mathbf{M}]+\mathbf{s}[\mathbf{C}]+[\mathbf{K}] \Leftarrow \text{system matrix} \quad (\mathbf{n} \text{ by } \mathbf{n}) \tag{9}$$

Equation (8) shows that any linear dynamic system has ***three basic parts***: applied forces (***inputs***), responses to those forces (***outputs***), and the dynamic system represented by its ***system matrix*** [B(s)].

Dynamic Model in Modal Coordinates

The modal parameters of a structure are the solutions to the homogeneous equations of motion. That is, when **{F(s)} = {0}** the solutions to equations (8) are complex valued eigenvalues and eigenvectors. The eigenvalues occur in complex conjugate pairs $\left(p_k, p_k^*\right)$. The eigenvalues are the solutions (or roots) of the characteristic polynomial, which is derived from the following determinant equation,

$$\mathbf{det}[\mathbf{B}(\mathbf{s})] = 0 \tag{10}$$

The eigenvalues (or ***poles***) of the system are:

$$\mathbf{p_k} = -\boldsymbol{\sigma}_\mathbf{k} + \mathbf{j}\boldsymbol{\omega}_\mathbf{k}, \qquad \mathbf{k} = \mathbf{1}, \dots \mathbf{m}$$
$$\mathbf{p_k^*} = -\boldsymbol{\sigma}_\mathbf{k} - \mathbf{j}\boldsymbol{\omega}_\mathbf{k}, \qquad \mathbf{k} = \mathbf{1}, \dots \mathbf{m}$$

$\mathbf{m}$ = number of modes

$\mathbf{p_k} = -\boldsymbol{\sigma}_\mathbf{k} + \mathbf{j}\boldsymbol{\omega}_\mathbf{k} \Leftarrow$ pole for the k^{th} mode

$\mathbf{p_k^*} = -\boldsymbol{\sigma}_\mathbf{k} - \mathbf{j}\boldsymbol{\omega}_\mathbf{k} \Leftarrow$ conjugate pole for the k^{th} mode

$\boldsymbol{\sigma}_\mathbf{k} \Leftarrow$ damping of the k^{th} mode

$\boldsymbol{\omega}_\mathbf{k} \Leftarrow$ damped natural frequency of the k^{th} mode, $\mathbf{k} = \mathbf{1}, \dots \mathbf{m}$

Each eigenvalue has a corresponding eigenvector, and hence the eigenvectors also occur in complex conjugate pairs, $(\{\mathbf{u_k}\}, \{\mathbf{u_k^*}\})$.

Each ***complex eigenvalue*** (also called a ***pole***) contains the modal frequency and damping. Each corresponding ***complex eigenvector*** is the mode shape.

Each eigenvector pair is a solution to the algebraic equations:

$$[\mathbf{B}(\mathbf{p_k})]\{\mathbf{u_k}\} = \{\mathbf{0}\} \quad \mathbf{k} = \mathbf{1}, \dots \mathbf{m} \quad (\mathbf{n}\text{-vector}) \tag{11}$$
$$[\mathbf{B}(\mathbf{p_k^*})]\{\mathbf{u_k^*}\} = \{\mathbf{0}\} \quad \mathbf{k} = \mathbf{1}, \dots \mathbf{m} \quad (\mathbf{n}\text{-vector}) \tag{12}$$

The eigenvectors (or ***mode shapes***), can be assembled into a matrix:

$$[\mathbf{U}] = [\{\mathbf{u}_1\}, \{\mathbf{u}_2\}, \dots, \{\mathbf{u_m}\}, \{\mathbf{u}_1^*\}, \{\mathbf{u}_2^*\}, \dots, \{\mathbf{u_m^*}\}] \Leftarrow \text{mode shape matrix} \quad (\mathbf{n} \text{ by } \mathbf{2m}) \tag{13}$$

This transformation of the equations of motion means that all vibration can be represented in terms of modal parameters.

Fundamental Law of Modal Analysis: All vibration is a ***summation of mode shapes***

Using the (**n** by **2m**) mode shape matrix **[U]**, the time domain response of a structure **{x(t)}** is related to its response in modal coordinates **{z(t)}** by

$$\{\mathbf{x}(\mathbf{t})\} = [\mathbf{U}]\{\mathbf{z}(\mathbf{t})\} \qquad (\mathbf{n}\text{-vector}) \qquad (14)$$

Applying the Laplace transform to equation (14) stated gives,

$$\{\mathbf{X}(\mathbf{s})\} = [\mathbf{U}]\{\mathbf{Z}(\mathbf{s})\}$$

where

$\{\mathbf{Z}(\mathbf{s})\} \leftarrow$ Laplace transform of displacements in modal coordinates (**2m**-vector)

Applying this transformation to equations (8) gives:

$$\left[\mathbf{s}^2[\mathbf{M}][\mathbf{U}] + \mathbf{s}[\mathbf{C}][\mathbf{U}] + [\mathbf{K}][\mathbf{U}]\right]\{\mathbf{Z}(\mathbf{s})\} = \{\mathbf{F}(\mathbf{s})\} \qquad (\mathbf{n}\text{-vector}) \qquad (15)$$

Pre-multiplying equation (15) by the ***transposed conjugate*** of the mode shape matrix ($[\mathbf{U}]^{\mathbf{t}}$) gives:

$$\left[\mathbf{s}^2[\mathbf{U}]^{\mathbf{t}}[\mathbf{M}][\mathbf{U}] + \mathbf{s}[\mathbf{U}]^{\mathbf{t}}[\mathbf{C}][\mathbf{U}] + [\mathbf{U}]^{\mathbf{t}}[\mathbf{K}][\mathbf{U}]\right]\{\mathbf{Z}(\mathbf{s})\} = [\mathbf{U}]^{\mathbf{t}}\{\mathbf{F}(\mathbf{s})\} \qquad (\mathbf{2m}\text{ by }\mathbf{2m}) \qquad (16)$$

Three new matrices can now be defined:

$[\mathbf{m}] = [\mathbf{U}]^{\mathbf{t}}[\mathbf{M}][\mathbf{U}] \leftarrow$ modal mass matrix (**2m** by **2m**) (17)

$[\mathbf{c}] = [\mathbf{U}]^{\mathbf{t}}[\mathbf{C}][\mathbf{U}] \leftarrow$ modal damping matrix (**2m** by **2m**) (18)

$[\mathbf{k}] = [\mathbf{U}]^{\mathbf{t}}[\mathbf{K}][\mathbf{U}] \leftarrow$ modal stiffness matrix (**2m** by **2m**)
(19)

The equations of motion ***transformed into modal coordinates*** now become

$$\left[\mathbf{s}^2[\mathbf{m}] + \mathbf{s}[\mathbf{c}] + [\mathbf{k}]\right]\{\mathbf{Z}(\mathbf{s})\} = [\mathbf{U}]^{\mathbf{t}}\{\mathbf{F}(\mathbf{s})\} (\mathbf{2m}\text{ by }\mathbf{2m}) \qquad (20)$$

Damping Models

In equation (1), the damping of the structure was modeled with a linear viscous force term which is proportional to surface velocity (1). This is called a **non-proportional damping** model. **Non-proportional damping** is the most commonly-used damping model, unless there is a known physical reason for using a different damping model.

If the structure model has **no damping ([C] = 0)**, then it can be shown that the modal mass & stiffness matrices are ***diagonal matrices*** and the equations of motion in modal coordinates (20) are ***uncoupled***.

If damping is modeled with a ***proportional damping matrix***, ($[\mathbf{C}] = \boldsymbol{\alpha}[\mathbf{M}] + \boldsymbol{\beta}[\mathbf{K}]$), where $\alpha \,\&\, \beta$ are proportionality constants, this is called a **proportional damping** model. With proportional damping, the modal mass, damping, & stiffness matrices are ***diagonal matrices***, and the equations of motion in modal coordinates (20) are ***again uncoupled***.

Lightly Damped Structures

When they vibrate, all real-world structures have ***several damping mechanisms*** which dissipate their vibration energy. On earth, the surrounding air always provides one damping mechanism. After all excitation forces are removed, all structural vibration will be damped out by the damping mechanisms.

A structure is assumed to be **lightly damped** if its ***damping forces are significantly less*** than its internal mass (inertial) and stiffness (restoring) forces.

If a structure exhibits troublesome resonance-assisted vibration, it is usually because it is lightly damped. A common way to define a lightly damped structure is,

A structure is called lightly damped if its modes have *less than 10 percent of critical damping*.

If a structure is lightly damping, then it can be shown that its modal mass, damping, & stiffness matrices in equation (20) are ***approximately diagonal matrices***. Furthermore, its mode shapes can be shown to be approximately ***normal*** (or ***real valued***). In this case, the **2m**-equations (20) are redundant, and can be replaced to **m**-equations, one corresponding to each mode.

The damping cases are summarized as follows.

Damping	**Mode Shapes**	**Modal Matrices**
None	Normal	Diagonal (m by m)
Non-Proportional	Complex	Non-Diagonal (2m by 2m)
Proportional	Normal	Diagonal (m by m)
Light	Almost Normal	Almost Diagonal (m by m)

Table 1. Damping Models

Scaling Mode Shapes to Unit Modal Masses

Mode shapes are called "***shapes***" because they are ***unique in shape***, but not in value. In other words, the mode shape vector $\{\mathbf{u}_k\}$ for each mode (**k**) does not have unique values. The "***shape***" of $\{\mathbf{u}_k\}$ is unique, but its shape values are arbitrary.

Another way of saying this is that the ratio of any two mode shape components is unique. A mode shape is also called an ***eigenvector***, meaning that its "***shape***" is unique, but its values are arbitrary. Therefore, a mode shape can be arbitrarily scaled using any scale factor.

Curve fitting a set of ***un-calibrated FRFs*** will yield ***un-scaled mode shapes***, hence they are ***not a modal model*** and cannot be used with SDM.

Modal Mass Matrix

SDM requires a modal model to describe the dynamics of the unmodified structure. In order to accurately model the structural dynamics, the mode shapes of the modal model must be scaled to preserve the mass, stiffness, & damping properties of the structure. SDM requires mode shapes which are scaled so that the ***modal masses are one or unity***. These are called UMM mode shapes.

When the mass matrix is post-multiplied by the mode shape matrix and pre-multiplied by its transpose, the result is the diagonal matrix shown in equation (21). ***This is a definition of modal mass***.

$$[\mathbf{U}]^t[\mathbf{M}][\mathbf{U}] = \begin{bmatrix} \ddots & & \\ & \mathbf{m} & \\ & & \ddots \end{bmatrix} = \begin{bmatrix} \ddots & & \\ & \frac{\mathbf{1}}{\mathbf{A\omega}} & \\ & & \ddots \end{bmatrix} \qquad (21)$$

where

$[\boldsymbol{M}]$ ← mass matrix (**n** by **n**)

$[\mathbf{U}] = [\{\mathbf{u}_1\},\{\mathbf{u}_2\},\ldots,\{\mathbf{u}_\mathbf{m}\}]$ ← mode shape matrix (**n** by **m**)

$\begin{bmatrix} \ddots & & \\ & \mathbf{m} & \\ & & \ddots \end{bmatrix} = \begin{bmatrix} \ddots & & \\ & \frac{\mathbf{1}}{\mathbf{A\omega}} & \\ & & \ddots \end{bmatrix}$ ← modal mass matrix (**m** by **m**)

The modal mass of each mode (**k**) is a diagonal element of the modal mass matrix.

$$\mathbf{m_k} = \frac{\mathbf{1}}{\mathbf{A_k\omega_k}} \leftarrow \text{modal mass} \qquad \mathbf{k=1},\ldots,\mathbf{m} \qquad (22)$$

$\mathbf{p_k = -\sigma_k + j\omega_k}$ ← pole location for the k^{th} mode

$\boldsymbol{\omega}_\mathbf{k}$ ← damped natural frequency of the k^{th} mode

$\mathbf{A_k}$ ← scaling constant for the k^{th} mode

Modal Stiffness Matrix

When the stiffness matrix is post-multiplied by the mode shape matrix and pre-multiplied by its transpose, the result is a diagonal matrix, shown in equation (23). ***This is a definition of modal stiffness.***

$$[\mathbf{U}]^t[\mathbf{K}][\mathbf{U}] = \begin{bmatrix} \ddots & & \\ & \mathbf{k} & \\ & & \ddots \end{bmatrix} = \begin{bmatrix} \ddots & & \\ & \frac{\boldsymbol{\sigma}^2+\boldsymbol{\omega}^2}{\mathbf{A\omega}} & \\ & & \ddots \end{bmatrix} \qquad (23)$$

where

$[\mathbf{K}]$ ← stiffness matrix. **(n** by **n)**

$$\begin{bmatrix} \ddots & & \\ & \mathbf{k} & \\ & & \ddots \end{bmatrix} = \begin{bmatrix} \ddots & & \\ & \frac{\sigma^2+\omega^2}{A\omega} & \\ & & \ddots \end{bmatrix} \leftarrow \text{modal stiffness matrix} \quad (\mathbf{m} \text{ by } \mathbf{m})$$

The modal stiffness of each mode (**k**) is a diagonal element of the modal stiffness matrix,

$$\mathbf{k_k} = \frac{\sigma_k^2+\omega_k^2}{A_k\omega_k} \leftarrow \text{modal stiffness} \qquad \mathbf{k}=\mathbf{1},\ldots,\mathbf{m} \tag{24}$$

where

$\boldsymbol{\sigma_k} \leftarrow$ modal damping of the k^{th} mode

Modal Damping Matrix

When the damping matrix is post-multiplied by the mode shape matrix and pre-multiplied by its transpose, the result is a diagonal matrix, shown in equation (25). ***This is a definition of modal damping.***

$$[\mathbf{U}]^t[\mathbf{C}][\mathbf{U}] = \begin{bmatrix} \ddots & & \\ & \mathbf{c} & \\ & & \ddots \end{bmatrix} = \begin{bmatrix} \ddots & & \\ & \frac{2\sigma}{A\omega} & \\ & & \ddots \end{bmatrix} \tag{25}$$

where

$[\mathbf{C}] \leftarrow$ damping matrix (**n** by **n**)

$$\begin{bmatrix} \ddots & & \\ & \mathbf{c} & \\ & & \ddots \end{bmatrix} = \begin{bmatrix} \ddots & & \\ & \frac{2\sigma}{A\omega} & \\ & & \ddots \end{bmatrix} \leftarrow \text{modal damping matrix} \quad (\mathbf{m} \textbf{ by } \mathbf{m})$$

The modal damping of each mode (**k**) is a diagonal element of the modal damping matrix,

$$\mathbf{c_k} = \frac{2\sigma_k}{A_k\omega_k}. \leftarrow \text{modal damping} \qquad \mathbf{k}=\mathbf{1},\ldots,\mathbf{m} \tag{26}$$

Unit Modal Masses

Each of the modal mass, stiffness, & damping matrix diagonal elements (22), (24), and (26) includes a ***scaling constant*** ($\mathbf{A_k}$). This constant is necessary because the ***mode shapes are not unique*** in value, and therefore can be arbitrarily scaled.

One of the common ways to scale mode shapes is to scale them so that the modal masses are ***"one"*** or ***"unity"***. Normally, if a mass matrix $[\mathbf{M}]$ were available, the mode vectors would simply be scaled such that when the triple product $[\mathbf{U}]^t[\mathbf{M}][\mathbf{U}]$ was formed, the resulting modal mass matrix would be an ***identity matrix***.

SDM Dynamic Model

The local eigenvalue modification process used by SDM requires a **modal model** of the ***unmodified*** structure. The modal model consists of the modal frequency, modal damping (optional), and mode shape of each mode in the model.

The dynamic model for the ***unmodified*** structure was given in equation (1). Similarly, the dynamic model for the ***modified*** structure is written:

$$[\mathbf{M} + \mathbf{\Delta M}]\{\ddot{\mathbf{x}}(\mathbf{t})\}+[\mathbf{C} + \mathbf{\Delta C}]\{\dot{\mathbf{x}}(\mathbf{t})\}+[\mathbf{K} + \mathbf{\Delta K}]\{\mathbf{x}(\mathbf{t})\} = \{\mathbf{f}(\mathbf{t})\} \qquad (27)$$

where

$[\mathbf{\Delta M}]$ 🡐 matrix of mass modifications (**n** by **n**)

$[\mathbf{\Delta C}]$ 🡐 matrix of damping modifications (**n** by **n**)

$[\mathbf{\Delta K}]$ 🡐 matrix of stiffness modifications (**n** by **n**)

SDM Equations Using UMM Mode Shapes

Unit Modal Mass (UMM) scaling is normally done on FEA mode shapes because the mass matrix is available for scaling them. However, when EMA mode shapes are extracted from experimental FRFs, no mass matrix is available for scaling the mode shapes to yield Unit Modal Masses.

The mode shapes are eigenvectors and hence ***have no unique values***, but if they are scaled so that the modal mass matrix is an ***identity matrix***, the equations of motion in modal coordinates (20) become:

$$\left[\mathbf{s}^{\mathbf{2}}[\mathbf{I}] + \mathbf{s}[\mathbf{2\sigma}] + [\mathbf{\Omega}^{\mathbf{2}}]\right]\{\mathbf{Z}(\mathbf{s})\} = [\mathbf{U}]^{\mathbf{t}}\{\mathbf{F}(\mathbf{s})\} \qquad (\mathbf{m}\text{-vector}) \qquad (28)$$

where

$[\mathbf{I}]$ 🡐 identity modal mass matrix (**m** by **m**)

$[\mathbf{2\sigma}]$ 🡐 diagonal modal damping matrix (**m** by **m**)

$[\mathbf{\Omega}^{\mathbf{2}}]$ 🡐 diagonal modal frequency matrix (**m** by **m**)

$[\mathbf{\Omega}^{\mathbf{2}}] = [\mathbf{\sigma}^{\mathbf{2}} + \mathbf{\omega}^{\mathbf{2}}]$

In Equation (28), the complete dynamics of the ***unmodified*** structure is represented by modal frequencies, modal damping, and mode shapes that are ***scaled to unit modal masses***. All mass, stiffness, & damping properties of the ***unmodified*** structure are preserved in the ***modal model*** that consists of UMM mode shapes

Using the UMM mode shapes, the equations of motion (27) for the ***modified*** structure can be transformed to modal coordinates,

$$\left[\mathbf{s}^2[\mathbf{m}] + \mathbf{s}[\mathbf{c}] + [\mathbf{k}]\right]\{\mathbf{Z}(\mathbf{s})\} = [\mathbf{U}]^{\mathbf{t}}\{\mathbf{F}(\mathbf{s})\} (\mathbf{m}\text{-vector}) \quad (29)$$

where

$$[\mathbf{m}] = [\mathbf{I}] + [\mathbf{U}]^{\mathbf{t}}[\boldsymbol{\Delta}\mathbf{M}][\mathbf{U}] \qquad (\mathbf{m} \text{ by } \mathbf{m}) \quad (30)$$

$$[\mathbf{c}] = [\mathbf{2}\boldsymbol{\sigma}] + [\mathbf{U}]^{\mathbf{t}}[\boldsymbol{\Delta}\mathbf{C}][\mathbf{U}] \qquad (\mathbf{m} \text{ by } \mathbf{m}) \quad (31)$$

$$[\mathbf{k}] = [\boldsymbol{\Omega}^{\mathbf{2}}] + [\mathbf{U}]^{\mathbf{t}}[\boldsymbol{\Delta}\mathbf{K}][\mathbf{U}] \qquad (\mathbf{m} \text{ by } \mathbf{m}) \quad (32)$$

For a lightly damped structure, the mode shapes are ***almost real-valued*** so the mode shape matrix has dimension (**n** by **m**).

The homogeneous form of equation (29) is solved by the SDM method to find the modal properties of the modified structure.

Using the approach of Hallquist, et al [2], an additional transformation of the modification matrices [ΔM],[ΔC],[ΔK] is made which results in a reformulation of the eigenvalue problem in modification space. For a single modification, this problem becomes a scalar eigenvalue problem, which can be solved quickly and efficiently. The drawback to making one modification at a time, however, is that if many modifications are required, computation time can become significant and errors will accumulate.

A more practical approach is to solve the homogeneous form of equation (29) directly. This is still a ***relatively small*** (**m** by **m**) eigenvalue problem which can include as many structural modifications as desired, but only needs to be solved once.

Equations (30) to (32) also indicate another advantage of SDM,

Only the mode shape components where the ***modification elements are attached*** to the structure model are required.

This means that only mode shape data for those DOFs ***where the modification elements are attached*** to the structure is necessary for SDM.

Scaling Residues to UMM Mode Shapes

Without a mass matrix, EMA mode shapes can be scaled to Unit Modal Masses by using the relationship between residues and mode shapes.

Residues are related to mode shapes by equating the numerators of curve fitting models (4) and (5),

$$[\mathbf{r}(\mathbf{k})] = \mathbf{A}_{\mathbf{k}}\{\mathbf{u}_{\mathbf{k}}\}\{\mathbf{u}_{\mathbf{k}}\}^{\mathbf{t}} \qquad \mathbf{k}=\mathbf{1},\ldots,\mathbf{m} \quad (33)$$

where

$[\mathbf{r}(\mathbf{k})]$ ← residue matrix for the mode **(k)** (**n** by **n**)

Residues are the numerators of the Transfer Function matrix in equation (4) when it is written in partial fraction form. For convenience, equation (4) is re-written here,

$$[\mathbf{H(s)}] = \sum_{k=1}^{m} \frac{[\mathbf{r(k)}]}{2j(s-p_k)} - \frac{[\mathbf{r(k)}]^*}{2j(s-p_k^*)} \tag{34}$$

* -denotes the ***complex conjugate***

Residues have engineering units associated with them and hence ***have unique values***. FRFs have units of (**motion/force**), and the FRF denominators have units of Hz or (**radians/second**). Therefore, the residues in the numerator have units of (**motion/force-seconds**).

Equation (34) can be written for the $\mathbf{j^{th}}$ **column** (or **row**) of the residue matrix and for mode (**k**) as,

$$\begin{Bmatrix} r_{1j}(k) \\ r_{2j}(k) \\ \cdot \\ \cdot \\ r_{jj}(k) \\ \cdot \\ r_{nj}(k) \end{Bmatrix} = A_k \begin{Bmatrix} u_{1k}u_{jk} \\ u_{2k}u_{jk} \\ \cdot \\ \cdot \\ (u_{jk})^2 \\ \cdot \\ u_{nk}u_{nk} \end{Bmatrix} = A_k u_{jk} \begin{Bmatrix} u_{1k} \\ u_{2k} \\ \cdot \\ \cdot \\ u_{jk} \\ \cdot \\ u_{nk} \end{Bmatrix} \qquad \mathbf{k=1,\ldots,m} \tag{35}$$

Unique **Variable** **Variable**

This relationship states that ***residues have unique values*** and preserve the physical properties of the structure, but ***mode shapes do not have unique values*** and therefore can be scaled in any manner.

The scaling constant $\mathbf{A_k}$ must be chosen so that equation (35) remains valid. Either the value of $\mathbf{A_k}$ can be chosen first, and the mode shapes scaled accordingly, or the mode shapes can be scaled first and $\mathbf{A_k}$ calculated so that equation (35) is still satisfied.

To obtain UMM mode shapes, simply set the ***modal mass equal to one*** and solve equation (22) for $\mathbf{A_k}$,

$$\mathbf{A_k} = \frac{1}{\omega_k} \qquad \mathbf{k=1,\ldots,m} \tag{36}$$

Driving Point FRF Measurement

Mode shapes scaled to Unit Modal Mass (**UMM mode shapes**) are obtained from the $\mathbf{j^{th}}$ column (or row) of the residue matrix by substituting equation (36) into equation (35),

$$\begin{Bmatrix} \mathbf{u}_{1k} \\ \mathbf{u}_{2k} \\ \cdot \\ \cdot \\ \cdot \\ \mathbf{u}_{nk} \end{Bmatrix} = \frac{\mathbf{1}}{\mathbf{A}_k \mathbf{u}_{jk}} \begin{Bmatrix} \mathbf{r}_{1j}(\mathbf{k}) \\ \mathbf{r}_{2j}(\mathbf{k}) \\ \cdot \\ \cdot \\ \cdot \\ \mathbf{r}_{nj}(\mathbf{k}) \end{Bmatrix} = \sqrt{\frac{\omega_k}{\mathbf{r}_{jj}(\mathbf{k})}} \begin{Bmatrix} \mathbf{r}_{1j}(\mathbf{k}) \\ \mathbf{r}_{2j}(\mathbf{k}) \\ \cdot \\ \cdot \\ \cdot \\ \mathbf{r}_{nj}(\mathbf{k}) \end{Bmatrix} \qquad \mathbf{k=1,\ldots, m} \qquad (37)$$

UMM
Mode Shape

The ***driving point residue*** $\mathbf{r}_{jj}(\mathbf{k})$ (where ***row index j*** equals ***column index j***), plays an important role in this scaling process. The driving point residue for each mode (**k**) is required in equation (37) for scaling mode shapes to UMM. Driving point residues are obtained by curve fitting a ***driving point FRF***.

A ***drive point FRF*** is any measurement where the excitation force DOF is the same as the response DOF.

Triangular FRF Measurements

In some cases, it is difficult or even impossible to make a good driving point FRF measurement. In those cases, an alternative set of measurements can be made from which to create UMM mode shapes. From equation (37) the following equation can be written,

$$\mathbf{u}_{jk} = \sqrt{\frac{\mathbf{r}_{jp}(\mathbf{k})\,\mathbf{r}_{jq}(\mathbf{k})}{\mathbf{A}_k\ \mathbf{r}_{pq}(\mathbf{k})}} \qquad \mathbf{k=1,\ldots, m} \qquad (38)$$

Equation (38) can be substituted for $\mathbf{u}_{jk}$ in equation (37) to calculate UMM mode shapes. To calculate a starting component $\mathbf{u}_{jk}$, three FRFs are required ($\mathbf{FRF_{jp}}$, $\mathbf{FRF_{jq}}$, $\mathbf{FRF_{pq}}$). **DOF(j)** is the (fixed) reference for the $\mathbf{j^{th}}$ column (or row) of FRF measurements, so the two measurements $\mathbf{FRF_{jp}}$ and $\mathbf{FRF_{jp}}$ would normally be made. In addition, one extra measurement $\mathbf{FRF_{pq}}$ is also required in order to obtain the three residues required by equation (38). Since the FRFs ($\mathbf{FRF_{jp}}$, $\mathbf{FRF_{jq}}$, $\mathbf{FRF_{pq}}$) form a triangle of ***off-diagonal FRFs*** in the FRF matrix, they are called a **triangular FRF measurement**. Equation (38) leads to the following conclusion,

A set of triangular FRF measurements which do not include driving point FRFs can be curve fit and their residues used to create **UMM mode shapes**.

Integrating Residues to Displacement Units

Vibration measurements are commonly made using either accelerometers that measure acceleration responses or vibrometers that measure velocity responses. Excitation forces are typically measured with a load cell. Therefore, FRFs calculated for experimental data will have units of either (**acceleration/force**) or (**velocity/force**).

Modal residues always have the units of the FRF multiplied by (**radians/second**).

- Residues extracted from FRFs with units of (**acceleration/force**) will have units of (**acceleration/force-seconds**)
- Residues extracted from FRFs with units of (**velocity/force**) will have units of (**velocity/force-seconds**)
- Residues extracted from FRFs with units of (**displacement/force**) will have units of (**displacement/force-seconds**)

Since the modal mass, stiffness, & damping equations (21), (23), and (25) assume **units of (displacement/force)**, residues with units of (**acceleration/force-seconds**) or (**velocity/force-seconds**) must be ***"integrated"*** to units of (**displacement/force-seconds**) units before scaling them to UMM mode shapes.

Integration of a time domain function has an equivalent operation in the frequency domain. Integration of a Transfer Function is done by dividing it by the Laplace variable(**s**),

$$[\mathbf{H_d(s)}] = \frac{[\mathbf{H_v(s)}]}{\mathbf{s}} = \frac{[\mathbf{H_a(s)}]}{\mathbf{s}^2} \tag{39}$$

where

$[\mathbf{H_d(s)}] \leftarrow$ transfer matrix in (**displacement/force**) units

$[\mathbf{H_v(s)}] \leftarrow$ transfer matrix in (**velocity/force**) units

$[\mathbf{H_a(s)}] \leftarrow$ transfer matrix in (**acceleration/force**) units

Since residues are the result of the partial fraction expansion form of an FRF, residues can be "***integrated***" directly using the formula,

$$[\mathbf{r_d(k)}] = \frac{[\mathbf{r_v(k)}]}{\mathbf{p_k}} = \frac{[\mathbf{r_a(k)}]}{(\mathbf{p_k})^2} \qquad \mathbf{k=1,\ldots,m} \tag{40}$$

where,

$[\mathbf{r_d(k)}] \leftarrow$ residue matrix in (**displacement/force**) units

$[\mathbf{r_v(k)}] \leftarrow$ residue matrix in (**velocity/force**) units

$[\mathbf{r_a(k)}] \leftarrow$ residue matrix in (**acceleration/force**) units

$\mathbf{p_k = -\sigma_k + j\omega_k} \leftarrow$ pole location for the $\mathbf{k^{th}}$ mode

If ***light damping*** *is assumed* and the ***mode shapes are real-valued***, equation (40) can be simplified to,

$$[\mathbf{r_d(k)}] = \mathbf{F_k}\ [\mathbf{r_v(k)}] = (\mathbf{F_k})^2\ [\mathbf{r_a(k)}] \tag{41}$$

where

$$\mathbf{F_k} \cong \frac{\boldsymbol{\omega_k}}{(\boldsymbol{\sigma}_\mathbf{k}^2 + \boldsymbol{\omega}_\mathbf{k}^2)} \qquad \mathbf{k=1},\ldots,\ \mathbf{m} \tag{42}$$

Equations (41) and (42) are summarized in the following table

To change Transfer Function units		Multiple Residues By
From	To	
$\frac{\text{ACCELERATION}}{\text{FORCE}}$	$\frac{\text{DISPLACEMENT}}{\text{FORCE}}$	$\mathbf{F}^2$
$\frac{\text{VELOCITY}}{\text{FORCE}}$	$\frac{\text{DISPLACEMENT}}{\text{FORCE}}$	$\mathbf{F}$

Table 2. Residue Scale Factors

where $\mathbf{F} \cong \dfrac{\boldsymbol{\omega}}{(\boldsymbol{\sigma}^2 + \boldsymbol{\omega}^2)}$ (**seconds**)

Effective Mass

A useful question to ask is,

"At one of its DOFs, what is the effective mass of a structure at one of its resonant frequencies?"

Another way to ask the question is,

"At one of its DOFs, if a structure were treated like an SDOF mass-spring-damper, what is its effective mass, effective stiffness & effective damping?"

The answer to those questions follows from a further use of the modal mass, stiffness, & damping equations (21), (23), and (25) and the definition **UMM mode shapes**.

It has already been shown that residues with units of *(***displacement/force-seconds***)* can be scaled to UMM mode shapes. One further assumption is necessary to define the effective mass at a DOF.

Diagonal Mass Matrix

If the mass matrix $\mathbf{[M]}$ is assumed to be a ***diagonal matrix***, then pre-multiplying & post-multiplying it by UMM mode shapes changes equation (21) to,

$$\sum_{\mathbf{j=1}}^{\mathbf{n}} \mathbf{mass}_{\mathbf{j}} \left(\mathbf{u}_{\mathbf{jk}}\right)^2 = \mathbf{1} \qquad \mathbf{k=1},\ldots,\ \mathbf{m} \tag{43}$$

where

$\mathbf{mass_j}$ ← $\mathbf{j^{th}}$ diagonal element of the mass matrix

$\mathbf{u_{jk}}$ ← $\mathbf{j^{th}}$ component of the UMM mode shape (**k**)

If the structure is viewed as a mass-spring-damper at DOF(**j**), the ***effective mass*** at the ***frequency of*** mode (**k**) at DOF(**j**) is determined from equation (43) as,

$$\mathbf{effective\,mass}_{\mathbf{j}} = \frac{1}{\left(\mathbf{u}_{\mathbf{jk}}\right)^2} \qquad \mathbf{j=1},\ldots,\ \mathbf{n} \tag{44}$$

If each DOF(**j**) is treated a driving point, equation (37) can be used to write the mode shape component $\mathbf{u}_{\mathbf{jk}}$ in terms of the modal frequency $\boldsymbol{\omega}_{\mathbf{k}}$ and driving point residue $\mathbf{r}_{\mathbf{jj}}(\mathbf{k})$,

$$\mathbf{u}_{\mathbf{jk}} = \sqrt{\boldsymbol{\omega}_{\mathbf{k}} \mathbf{r}_{\mathbf{jj}}(\mathbf{k})} \qquad \mathbf{j=1},\ldots,\ \mathbf{n} \tag{45}$$

Substituting equation (45) into equation (44) gives another expression for the effective mass at the frequency of mode (**k**),

$$\mathbf{effective\ mass}_{\mathbf{j}} = \frac{\mathbf{1}}{\boldsymbol{\omega}_{\mathbf{k}} \mathbf{r}_{\mathbf{jj}}(\mathbf{k})} \qquad \mathbf{j=1},\ldots,\ \mathbf{n} \tag{46}$$

Checking the Engineering Units

Assuming that the driving point residue $\mathbf{r}_{\mathbf{jj}}(\mathbf{k})$ has units of ***(displacement/force-seconds)*** as discussed earlier, and the modal frequency $\boldsymbol{\omega}_{\mathbf{k}}$ has units of ***(radians/second)***, then the effective mass would have units of (**force-sec^2/displacement**)**,** which are units of mass.

Using the **effective mass**, the **effective stiffness & damping** of the structure can be calculated using equations (29) and (31).

Effective Mass Example

Suppose that we have the following data for a single mode of vibration,

Frequency = 10.0 Hz.

Damping = 1.0 %

$$\textbf{Residue Vector} = \begin{Bmatrix} -0.1 \\ +2.0 \\ +0.5 \end{Bmatrix}$$

Also, suppose that the FRF measurements that were curve fit to obtain this data have units of (**Gs/Lbf**). Also assume that the driving point is at the second DOF of the residue vector, and therefore driving point residue = 2.0.

Converting the frequency & damping into units of **radians/second**,

Frequency = 62.83 Rad/Sec

Damping = 0.628 Rad/Sec

The residues always carry the units of the FRF measurement multiplied by (**radians/second**). For this example, the units of the residues are,

Residue Units ➔ Gs/(Lbf-Sec) ➔ 386.4 Inches/(Lbf-Sec^3)

In these units, the residues become,

$$\textbf{Residue Vector} = \begin{Bmatrix} -38.64 \\ +772.8 \\ +193.2 \end{Bmatrix} \qquad \textbf{Inches/(Lbf-Sec}^3\textbf{)}$$

Since the modal mass, stiffness, & damping equations (21), (23), and (25) assume units of (**displacement/force**), the above residues with units of (**acceleration/force**) must be converted to (**displacement/force**) units. This is done by using the appropriate scale factor from Table 2. For this example:

$$\mathbf{F}^2 \cong \left(\frac{1}{62.83}\right)^2 = 0.000253 \qquad (\textbf{Seconds}^2)$$

Multiplying the residues by $\mathbf{F}^2$ gives,

$$\textbf{Residue Vector} = \begin{Bmatrix} -0.00977 \\ +0.1955 \\ +0.0488 \end{Bmatrix} \qquad \textbf{Inches/(Lbf-Sec)}$$

Using equation (37) the **residue mode shape** must be multiplied by the following scale factor to obtain a UMM mode shape,

$$\mathbf{SF} = \sqrt{\frac{\omega}{r_{jj}}} = \sqrt{\frac{62.83}{+0.1955}} = \mathbf{17.927}$$

Therefore,

$$\textbf{UMM Mode Shape} = \begin{Bmatrix} -0.175 \\ +3.505 \\ +0.875 \end{Bmatrix} \quad \textbf{Inches/(Lbf-Sec)}$$

Using equation (44), the **effective mass** at the driving point is,

$$\textbf{effective mass} = \frac{1}{(u_2)^2} = \frac{1}{(3.505)^2} = \mathbf{0.0814} \qquad \textbf{Lbf-sec}^2\textbf{/in.}$$

Or, using equation (46), the **effective mass** at the driving point is,

$$\textbf{effective mass} = \frac{1}{\omega\ r_{22}} = \frac{1}{(62.83)(0.1955)} = \mathbf{0.0814} \ \ \textbf{Lbf-sec}^2\textbf{/in.}$$

SDM Example

In this example, SDM will be used to model the attachment of a RIB stiffener to an aluminum plate. The new mode shapes obtained from SDM will be compared with the FEA mode shapes of the plate with the RIB attached, and with the EMA mode shapes obtained from an impact test of the actual plate with the RIB attached. Mode shapes will be compared in three cases.

1. **EMA versus FEA** mode shapes of the plate ***without the RIB***
2. **SDM versus FEA** mode shapes of the plate ***with the RIB attached***
3. **SDM versus EMA** mode shapes of the plate ***with the RIB attached***

The plate and RIB are shown in Figure 5. The dimensions of the plate are 20 inches (508 mm) by 25 inches (635 mm) by 3/8 inches (9.525 mm) thick. The dimensions of the RIB are 3 inches (76.2 mm) by 25 inches (635 mm) by 3/8 inches (9.525 mm) thick.

Two roving impact modal tests were conducted on the plate, one before and one after the RIB stiffener was attached to the plate. FRFs were calculated from the impact force and the acceleration response only in the vertical (Z-axis) direction.

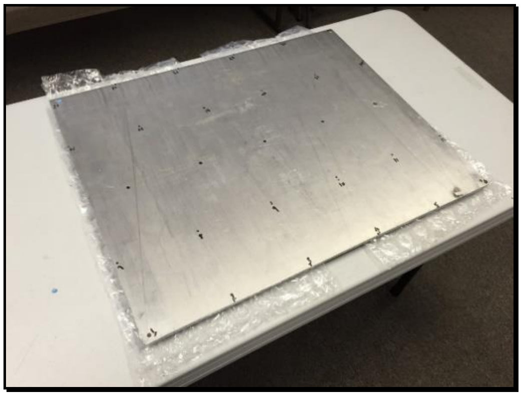

Figure 5A. Aluminum Plate

Figure 5B. RIB and Cap Screws

Figure 5C. Plate and RIB Attached

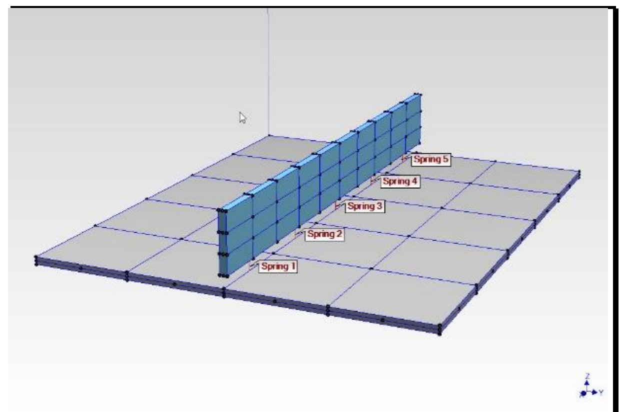

Figure 6. FEA Springs Modeling the Cap Screws

Cap Screw Stiffnesses

The RIB stiffener was attached to the plate with five cap screws, shown in Figure 5B. When the RIB is attached to the plate, ***translational & torsional forces*** are applied between the two substructures along the length of the plate centerline where they are attached together. Both ***translational & torsional stiffness forces*** must be modeled in order to represent the real-world plate with the RIB stiffener attached.

The joint stiffness was modeled using **six-DOF springs** located at the five cap screw locations, as shown in Figure 6. Each six-DOF FEA spring model contains ***three translational*** **DOFs** and ***three rotational*** **DOFs**. The six-DOF FEA springs were given large stiffness values to model a tight fastening of RIB to the plate using the cap screws.

- Translational stiffness: ***1 x E6 lbs/in*** (***1.75E+05 N/mm***)
- Torsional stiffness: ***1 x E6 in-lbs/degree*** (***1.75E+05 mm-N/degree***)

EMA Mode Shapes of the Plate

FRFs were calculated from data acquired while impacting the plate in the vertical direction, at each of the 30 points shown in Figure 7. The plate was supported on bubble wrap laying on top of a table as shown in Figure 5. A fixed reference accelerometer was attached to the plate. (The location of the reference accelerometer is arbitrary.)

The EMA modal parameters were estimated by curve fitting the 30 FRFs calculated from the roving impact test data. EMA mode shapes for 14 modes were obtained by curve fitting the FRFs, each mode shape having 30 DOFs (1Z through 30Z). A curve fit on one of the FRFs is shown in Figure 4.

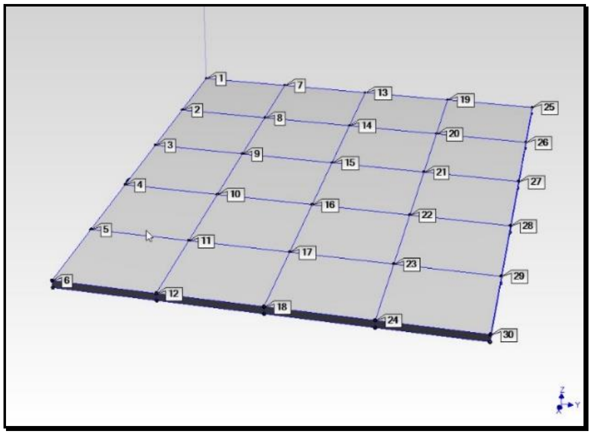

Figure 7. Impact Test Points

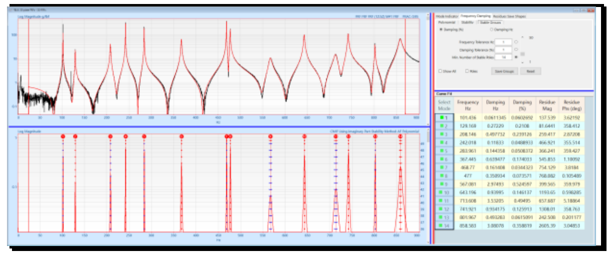

Figure 8. Curve of an Experimental FRF

FEA Mode Shapes of the Plate

An FEA model of the plate was constructed using ***80 FEA plate (membrane) elements***. The following properties of the aluminum material in the plate were used,

1. **Young's modulus of elasticity:** 1E7 lbf/in^2 (6.895E4 N/mm^2)
2. **Density:** 0.101 lbm/in^3 (2.796E-6 kg/mm^3)
3. **Poisson's Ratio:** 0.33.
4. **Plate thickness:** 0.375 in (9.525 mm)

The FEA model shown in Figure 9 has 99 points (or nodes). The eigen-solution included the first 20 FEA modes, **6 rigid-body mode shapes** and **14 flexible-body mode shapes**. Each FEA mode shape has **594 DOFs** (3 translational & 3 rotational DOFS at each point). The FEA mode shapes were scaled to UMM mode shapes, hence they constitute a ***modal model*** of the plate.

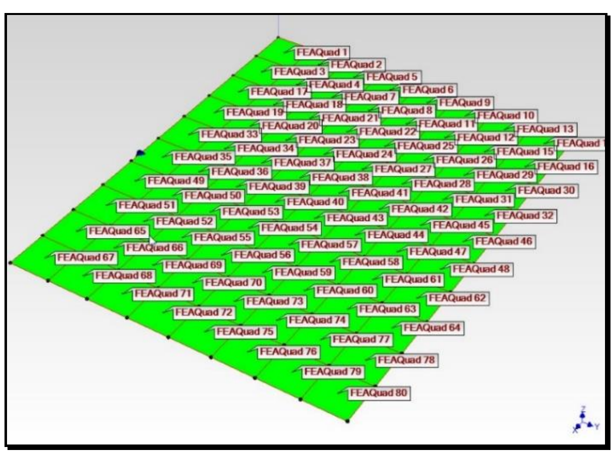

Figure 9. FEA Model with FEA Quads

Mode Shape Comparison

The Modal Assurance Criterion (**MAC**) values between each EMA mode shape and each **flexible-body** FEA mode shape are displayed in the bar chart in Figure 9.

MAC is a measure of the co-linearity of two mode shapes. The following rule-of-thumb is commonly used with MAC

- MAC = 1.00 ➔ two shapes are the same (they lie on the same straight line)
- MAC >= 0.90 ➔ two shapes are similar
- MAC <= 0.90 ➔ two shapes are different

The diagonal MAC bars in Figure 9 indicate that each flexible-body EMA mode shape ***closely matched one-for-one*** with the each flexible-body FEA mode shape. The ***worst-case pair*** of matching mode shapes is the first pair with **MAC = 0.97**.

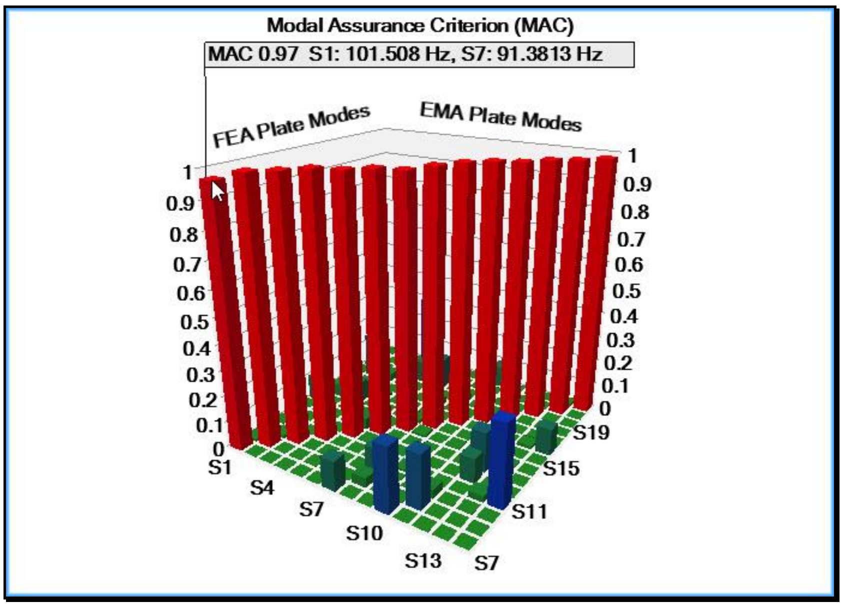

Figure 10. MAC Between FEA & EMA Mode Shapes

Modal Frequency Comparison

The modal frequencies of the matching FEA & EMA mode pairs are listed in Table 3. Each EMA modal frequency is ***higher*** than the frequency of its corresponding FEA mode. The pair with the highest difference is different by 100 Hz.

Shape Pair	FEA Frequency (Hz)	EMA Frequency (Hz)	EMA Damping (Hz)	MAC
1	91.4	102	0.031	0.968
2	115	129	0.250	0.991
3	190	208	0.458	0.990
4	217	242	0.107	0.993
5	251	284	0.106	0.984
6	332	367	0.642	0.985
7	412	469	0.159	0.975
8	424	477	0.339	0.985
9	496	567	3.130	0.991
10	564	643	0.936	0.991
11	626	714	3.680	0.984
12	654	742	0.923	0.987
13	689	802	0.443	0.983
14	757	859	3.090	0.984

Table 3. FEA versus EMA Modes-Plate without RIB

The frequency differences indicate that the stiffness of the actual aluminum plate ***is greater than*** the stiffness of the FEA model. These frequency differences could be reduced by ***increasing the modulus of elasticity*** or ***increasing the thickness*** of the FEA plate elements. However, since the EMA and FEA modes shapes are closely-matched, the EMA frequency & damping can be combined with the FEA mode shapes to provide a more accurate modal model of the plate.

Hybrid Modal Model

In most cases, EMA mode shapes will not have as many DOFs in them as FEA mode shapes. But in most all cases, EMA mode shapes with have more accurate modal frequencies than FEA mode shapes. Also, EMA mode shapes always have non-zero modal damping, whereas FEA mode shapes typically have no damping.

If a pair of EMA & FEA mode shapes is highly correlated (their MAC value is ***close to 1.0***), a hybrid mode shape can be created by replacing the frequency & damping of each FEA mode shape with the frequency & damping of its ***closely-matching*** EMA mode shape.

In a ***Hybrid mode shape,*** the frequency & damping of each FEA mode shape is replaced with the frequency & damping of its ***closely-matching*** EMA mode shape.

In Figure 10 and Table 3, each FEA mode shape has a ***high MAC value*** with a corresponding EMA mode shape. Therefore, a hybrid modal model of the plate can be created by replacing the modal frequency & damping of each FEA mode shape with the modal frequency & damping of its closely-matching EMA mode shape.

A ***hybrid modal model*** has several advantages for modeling the dynamics of an ***unmodified*** structure with SDM,

- Its modal frequencies & damping are more realistic
- It can have DOFs at locations where EMA data was not acquired
- Its mode shapes can include ***rotational*** **DOFs** which are not typically included in EMA mode shapes
- FEA mode shapes are typically scaled to UMM mode shapes

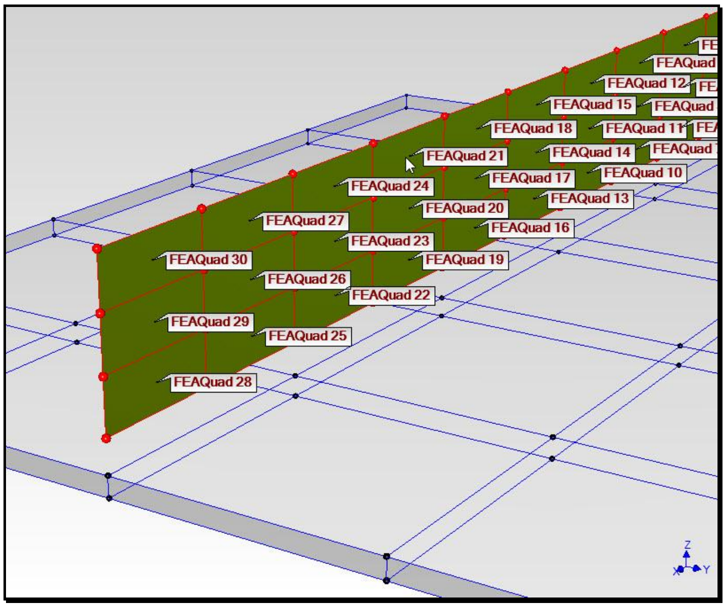

Figure 11. FEA RIB Model

RIB FEA Model

An FEA model of the RIB in a free-free condition (no fixed boundaries) was created using 30 FEA Quad Plate elements. The FEA RIB model is shown in Figure 11.

The frequencies of the first 16 FEA modes of the RIB are listed in Table 4. Because it has free-free boundary conditions, the ***first six modes*** of the FEA model are ***rigid-body*** **mode shapes** with zero **“0”** frequency. These FEA mode shapes are UMM mode shapes, so they constitute a modal model of the RIB.

Shape Pair	FEA Frequency (Hz)	EMA Frequency (Hz)	EMA Damping (Hz)
1	0.0		
2	0.0		
3	0.0		
4	0.0		
5	0.0		
6	0.0		
7	117.0	121.0	0.78
8	315.0	330.0	0.72
9	521.0	582.0	0.89
10	607.0	646.0	2.49
11	987.0	1.07E+03	3.86
12	1.07E+03	1.18E+03	1.24
13	1.45E+03	1.60E+03	8.72
14	1.67E+03	1.79E+03	2.55
15	1.99E+03	2.24E+03	3.92
16	2.32E+03	2.44E+03	2.97

Table 4. FEA vs. EMA RIB Frequencies

RIB Impact Test

The RIB was impact tested to obtain its EMA modal frequencies & damping, but not its mode shapes. The RIB was only impacted once, and the resulting FRF was curve fit to obtain its EMA modal frequencies & damping. The curve fit of the FRF measurement is shown in Figure 12, and the resulting EMA frequencies & damping are listed in Table 4.

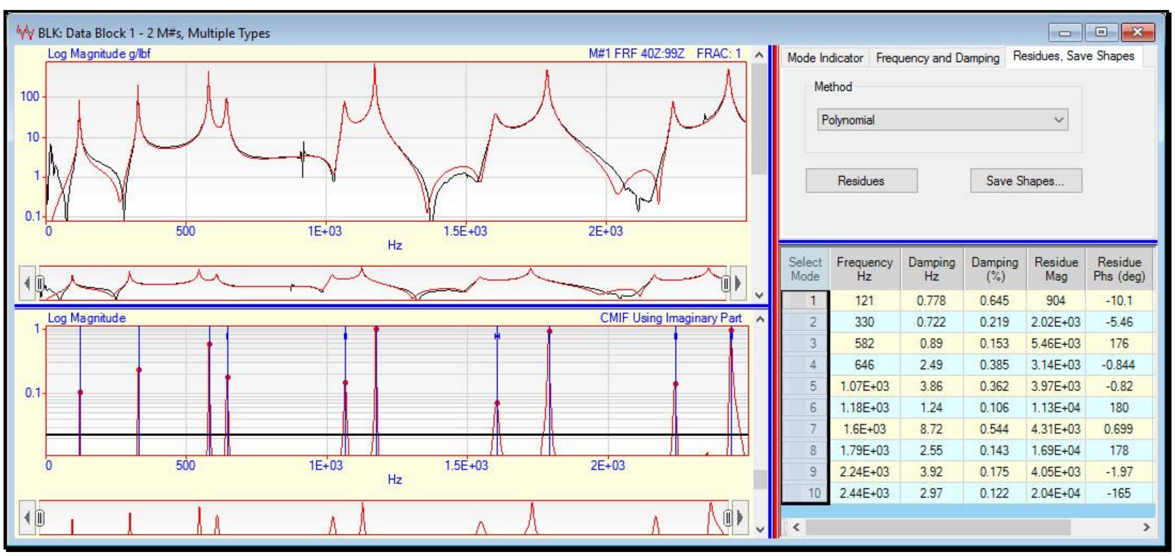

Figure 12. Curve Fit of a RIB FRF.

Hybrid Modal Model of the RIB

We have already seen that pairs of the EMA & FEA mode shapes of the plate are ***strongly correlated*** based upon their ***high MAC values***. The only significant difference between the EMA & FEA mode shapes was their modal frequencies, and each EMA mode also has modal damping while the FEA mode shapes do not.

Before it is attached to the plate, the RIB is a free-body in space. It is essential that the ***rigid-body modes*** of the RIB be included in its modal model to correctly model its free-body dynamics. Rigid-body modes are typically not measured experimentally but they are including in the FEA mode shapes.

A RIB **hybrid modal model** was created by replacing the frequency & damping of each FEA mode shape with the EMA modal frequency & damping from its closely-matching EMA mode shape. The six rigid-body FEA mode shapes were also retained in the hybrid modal model to define the free-body dynamics of the RIB.

Substructure Modal Model

In order to model the RIB attached to the plate using SDM, the Hybrid modal model of the RIB was added to the Hybrid modal model of the plate to create a modal model for the entire ***unmodified*** structure. This is called a ***substructure modal model***.

Figure 13 shows how the points on the RIB are ***numbered differently*** than the points on the plate. This ensures that the DOFs of the RIB modes are ***uniquely numbered*** compared to the DOFs of the plate modes.

Block Diagonal Format

When the modal model of the RIB is added to the modal model of the plate, the unique numbering of the points on the plate and RIB creates a modal model in ***block diagonal format***. In block diagonal format, the DOFs of the RIB mode shapes are ***zero valued*** for DOFs on the plate, and likewise the DOFs of the plate mode shapes are ***zero valued*** for the DOFs of the RIB.

The ***plate modal model*** contains 14 modes with 594 DOFs (297 translational and 297 rotational DOFs) in each mode shape. The ***RIB modal model*** contains 16 modes with 264 DOFs (132 translational and 132 rotational DOFs) in each mode shape. Therefore, the ***substructure modal model*** contains 30 modes and 858 DOFs (429 translational and 429 rotational DOFs) in each mode shape.

Calculating New Modes with SDM

The five FEA springs shown in Figure 13 were used by SDM to model the five cap screws that attach the RIB to the plate. These springs were used together with the ***substructure modal model*** for the unmodified structure as inputs to SDM.

Even though the mode shapes in the substructure modal model have 858 DOFs in them, only the mode shape DOFs at the attachment points of the FEA springs are used by SDM to calculate the new frequencies & damping of the plate with the RIB attached. Following that, all 858 DOFs of the unmodified mode shapes are used to calculate the new mode shapes of the modified structure.

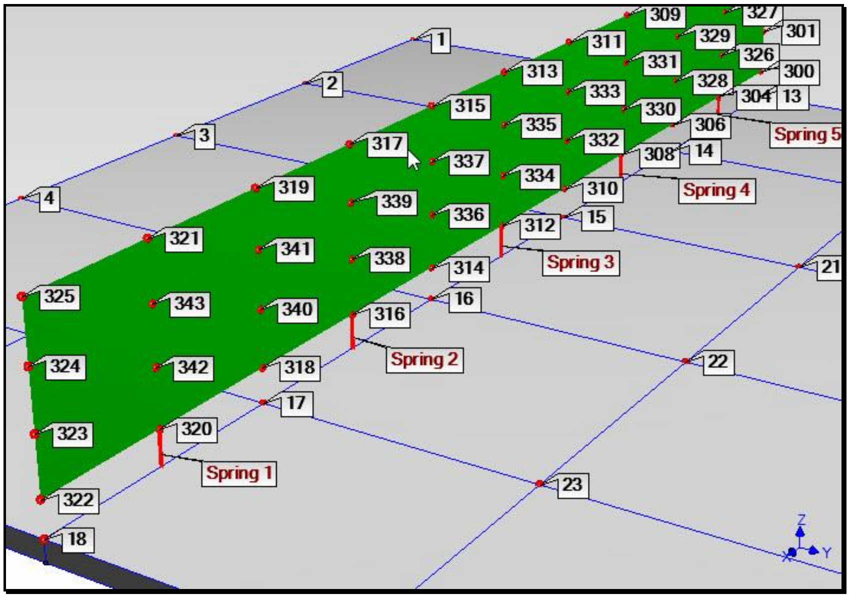

Figure 13. Point numbers of the Plate and RIB

SDM versus FEA Modes-Plate and RIB

An FEA model consisting of the 80 quad plate elements of the plate, 30 quad plate elements of the RIB, and the 5 springs was also solved using an FEA eigen-solver. The SDM & FEA results are compared in Table 5.

Shape Pair	FEA Frequency (Hz)	SDM Frequency (Hz)	SDM Damping (Hz)	MAC
1	96.0	108.2	0.035	1.00
2	170.5	187.6	0.369	0.99
3	222.6	253.3	0.118	0.98
4	232.7	311.5	0.293	0.92
5	245.1	351.7	0.104	0.98
6	415.0	479.2	0.171	0.98
7	423.0	521.3	0.713	0.91
8	459.1	537.4	2.770	0.95
9	530.7	619.1	0.863	0.91
10	596.0	1412.0	3.185	0.63

Table 5. SDM Modes versus FEA Modes-Plate with RIB

The ***first nine pairs of mode shapes*** in Table 5 have MAC values ***greater than 0.90***, indicating a ***strong correlation*** between those SDM and FEA mode shapes. The FEA modal frequencies are lower than the SDM frequencies for those ***first nine mode shape pairs***.

It will be shown later in **FEA Model Updating** how SDM can be used to find more realistic material properties for the FEA model so that its modal frequencies more closely match the EMA frequencies.

SDM Mode Shapes

Figure 14 is a display of the first ten SDM mode shapes. Five of the ten mode shapes ***clearly reflect the torsional coupling*** between the RIB and the plate. All ten mode shapes show the intended effect of the RIB stiffener on the plate.

All bending of the plate along its centerline ***has been eliminated*** by attaching the RIB to it.

Both the RIB and plate are flexing together in unison, both being influenced by the torsional stiffness created by the 6-DOF springs that modeled the cap screws.

Attaching the RIB to the plate has created new modes with mode shapes that ***did not exist before the modification***. This confirms the law stated earlier.

Fundamental Law of Modal Analysis: All vibration is a ***summation of mode shapes***

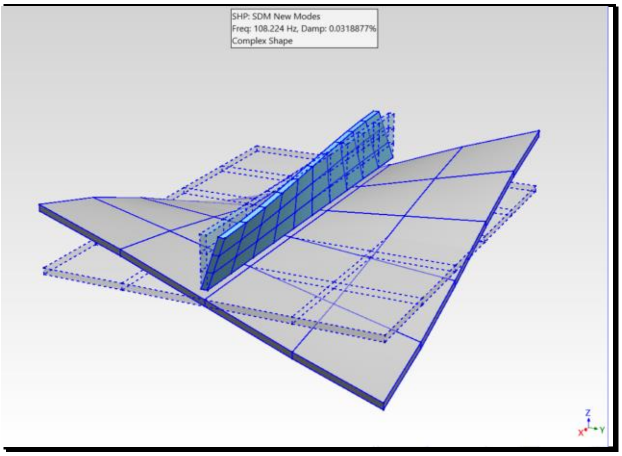

SDM Mode Shape 1

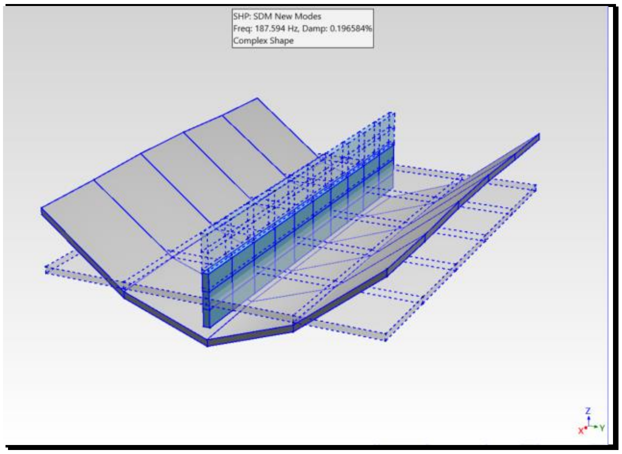

SDM Mode Shape 2

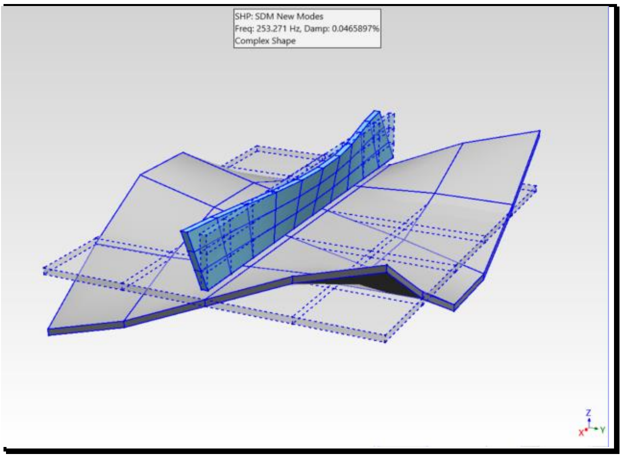

SDM Mode Shape 3

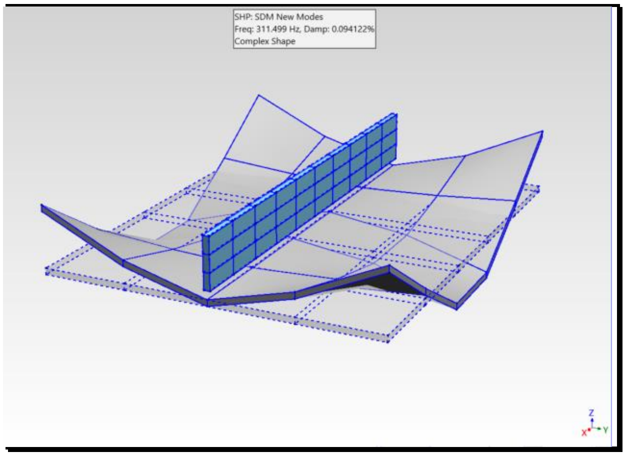

SDM Mode Shape 4

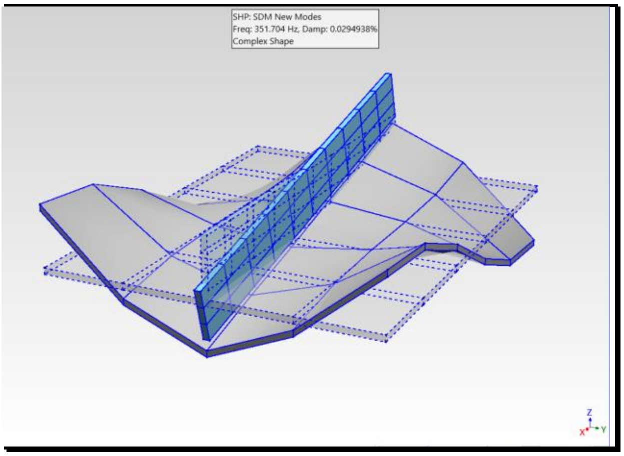

SDM Mode Shape 5

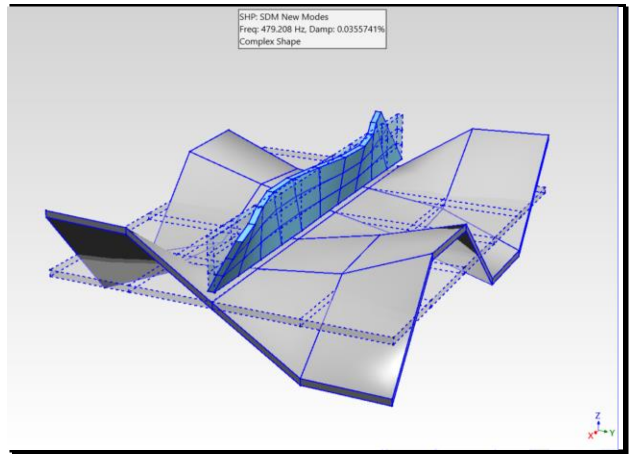

SDM Mode Shape 6

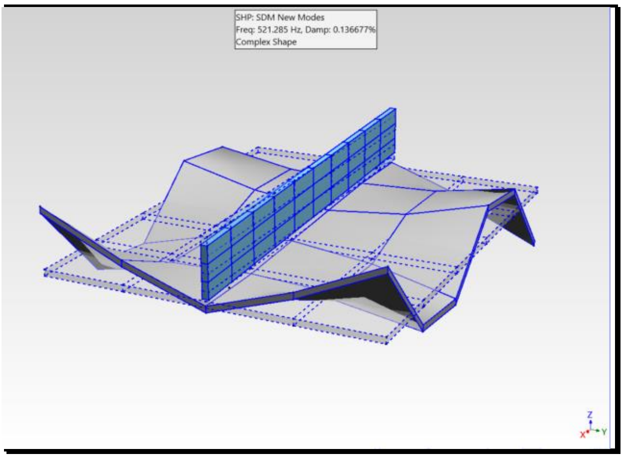

SDM Mode Shape 7

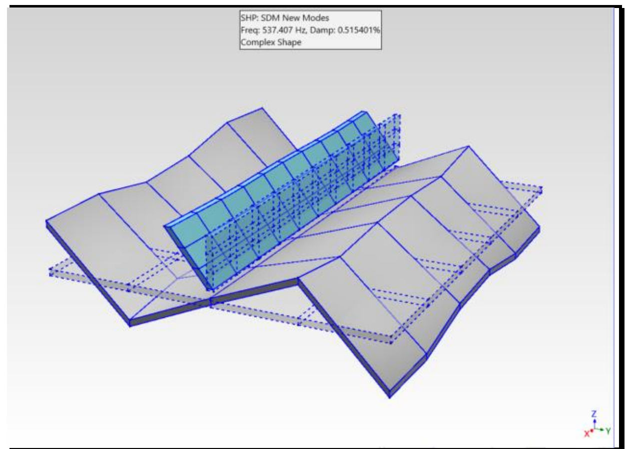

SDM Mode Shape 8

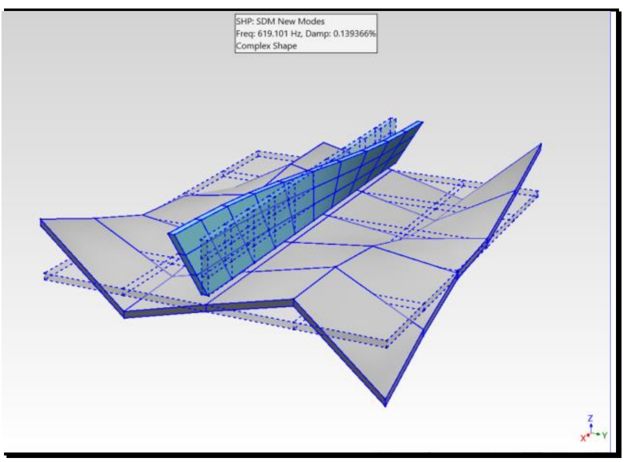

SDM Mode Shape 9

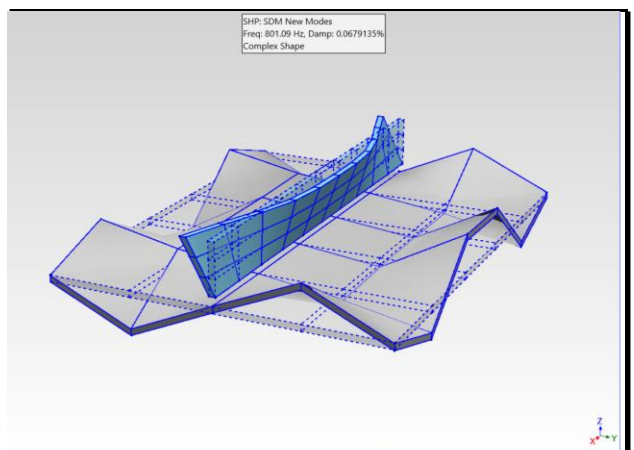

SDM Mode Shape 10

Figure 14. SDM Mode Shapes

SDM versus EMA Modes-Plate and RIB

To compare the SDM mode shapes with EMA mode shapes, the plate with the RIB attached was impact tested using a roving impact hammer. The plate was impacted at 24 points on the plate in the **(vertical) Z-direction**, as shown in Figure 15. This provided enough EMA mode shape data for comparison with the SDM mode shapes.

A driving point FRF measurement is not required since the EMA mode shapes do not require UMM scaling to compare them with SDM mode shapes using MAC.

The curve fit of a typical FRF from the impact test is shown in Figure 16. The 24 FRFs were curve fit to extract the EMA mode shapes for the modified plate.

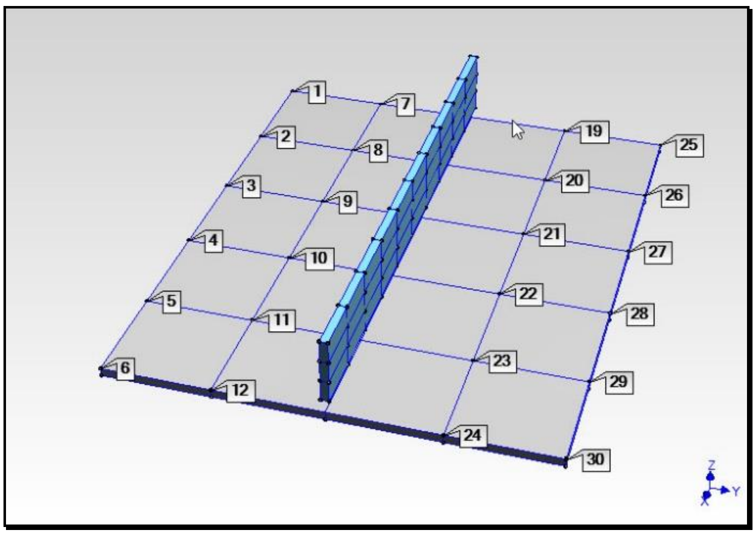

Figure 15. Impact Points on Plate with RIB

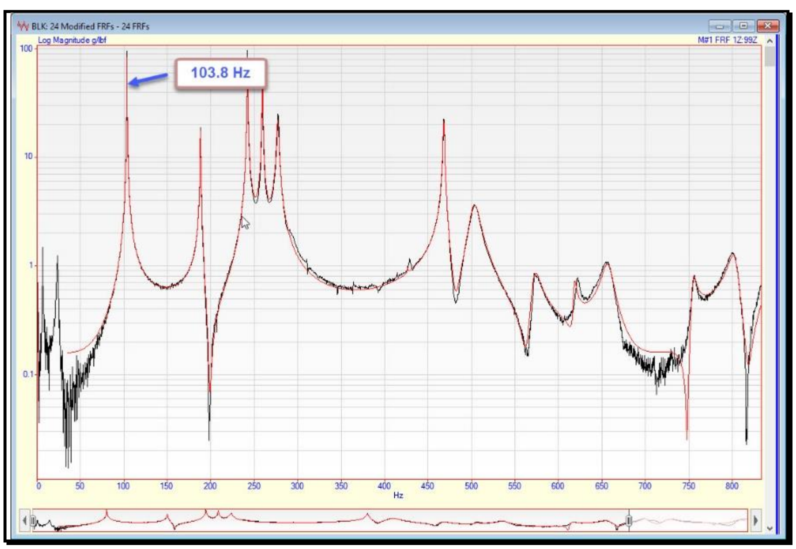

Figure 16. Curve Fit of an FRF from the Plate with RIB

Shape Pair	EMA Frequency (Hz)	EMA Damping (Hz)	SDM Frequency (Hz)	SDM Damping (Hz)	MAC
1	103.8	0.142	108.2	0.034	0.99
2	188.5	0.377	187.6	0.369	0.99
3	242.5	0.254	253.3	0.118	0.99
4	277.8	0.941	311.5	0.293	0.98
5	259.8	0.254	351.7	0.104	0.97
6	468.6	0.710	479.2	0.171	0.98
7	504.1	6.202	521.3	0.713	0.97
8	572.5	1.877	537.4	2.770	0.97
9	620.3	0.818	619.1	0.865	0.85
10	803.3	6.070	801.1	0.544	0.86

Table 6. EMA versus SDM modes for the Plate and RIB

Conclusions

In Table 6, the modal frequencies of the ***first three*** SDM modes agree closely with the frequencies of the first three EMA modes. In Table 6, the ***first eight*** SDM mode shapes agree closely with the first eight EMA mode shapes, all having MAC values ***close to 1.0***.

The ***close agreement*** between the ***first eight*** mode shapes from all three cases; SDM, FEA, & EMA, verify that the joint stiffness provided by the five cap screws was correctly modeled in SDM using 6-DOF springs and mode shapes with rotational DOFs in them. This example has demonstrated that even with the use of a ***truncated modal model*** containing relatively few mode shapes, SDM provides realistic and useful results.

Several options could be explored to obtain closer agreement between the SDM, FEA, & EMA mode shapes,

- Add more FEA springs between the RIB and the plate to model the stiffness forces between the two substructures
- Use more FEA quad plate elements for the plate and RIB. Increasing the mesh of nodes for the plate elements usually provides more accurate FEA mode shapes.
- Include more modes in the modal model of the ***unmodified*** plate and RIB. Extra modes will provide a more complete dynamic model of the two substructures as input to SDM.

Modeling a Tuned Vibration Absorber with SDM

Another use of SDM is to model the addition of tuned mass-spring-damper vibration absorbers to a structure. A tuned vibration absorber is designed to absorb some of the vibration energy in the structure so that one of its modes of vibration will absorb less energy and hence the structure will vibrate with less overall amplitude.

A tuned absorber is used to ***suppress resonant vibration*** in a structure. The primary effect of adding a tuned absorber is to ***replace one of its resonances*** with ***two lower amplitude resonances***.

The mass and stiffness of the tuned absorber is chosen so that its natural frequency is ***"close to"*** the resonant frequency of a structural resonance to be suppressed. Ideally, the absorber should be attached to the structure at a point and in a direction where the magnitude of the resonance is large, near an ***anti-node*** of its mode shape. The absorber will have no effect if attached at a ***node*** of the mode shape, where its magnitude is zero.

SDM models the attachment of a tuned absorber to a structure by solving a sub-structuring problem like the one in the previous plate and RIB example. A tuned absorber is modeled by attaching an FEA mass to the structure using an FEA spring & FEA damper. SDM solves for the new modes of the structure with the tuned vibration absorber attached.

To begin the design, a mass must be chosen for the tuned absorber. The following rule should be used in choosing an absorber mass.

Rule of Thumb: The mass of a tuned absorber should not exceed **10%** of the mass of the structure.

After the mass has been chosen, the frequency of the structural mode to be suppressed together with the mass of the absorber will determine the stiffness of the spring required to attach the absorber to the structure. These three values are related to one another by the formula,

$$\mathbf{k} = \mathbf{m}\ \boldsymbol{\omega}^{2} \qquad (47)$$

where

$\mathbf{m}$ ← tuned absorber mass

$\boldsymbol{\omega}$ ← frequency of the structural mode to be suppressed

$\mathbf{k}$ ← tuned absorber stiffness

Adding a damper is optional. If a damper is added between the absorber mass and the structure, its damping value must also be chosen. A realistic damping value of a ***few percent of critical damping*** is calculated using the following formulas.

$$\mathbf{k} = \mathbf{m}\ (\boldsymbol{\omega}^{2} + \boldsymbol{\sigma}^{2}) \qquad (48)$$

where

$\boldsymbol{\sigma} = \dfrac{\boldsymbol{\omega}}{\sqrt{1-\%^{2}}}$ ← damping decay constant

% ← percent of critical damping

The mode shape of the unattached tuned absorber is simply the UMM rigid-body mode shape of the mass substructure in free-space. In order to use SDM to model a tuned absorber, two more steps are necessary,

1. The free-free mode shape of the tuned absorber must be added in ***block diagonal format*** to the mode shapes of the unmodified structure. The block diagonal format was explained in the previous plate and RIB example
2. The attachment DOF (point & direction) of the tuned absorber must be defined. A geometric model of the structure is usually required for this

Adding a Tuned Absorber to the Plate and RIB

SDM will be used to model the attachment of a tuned vibration absorber to one corner of the flat aluminum plate used in the previous example. The absorber will be designed to suppress the amplitude of the high-Q resonance at 108 Hz, shown in the **blue FRF magnitude** plot in Figure 17.

The plate and RIB weighs about **21.3 lbm** (**9.7 kg**). For this example, the absorber weight is chosen as **0.5 lbm** (**0.23 kg**). In order to absorb energy from the plate and RIB at 108 Hz, the attachment spring stiffness must be chosen so that the absorber will resonate at 108 Hz.

The absorber parameters are,

Mass: **0.5 lbm** (**0.23 kg**)
Stiffness: **586.6 lbf/in** (**104.8 N/mm**)
Damping: **0.5%**

Only the modal model data of the unmodified plate and RIB at **DOF 1Z** is required. Since the mass will be attached to the plate and RIB as a substructure, the mode shape of the free-body mass is added to the mode shapes of the unmodified plate and RIB in ***block diagonal format***, explained in the previous example.

To model the tuned absorber, the modal model for the ***unmodified*** plate and RIB substructure together with a modal model and the spring & damper of the absorber are used as inputs to SDM. SDM then solves for the new modes of the plate and RIB with the absorber mass attached by the spring & damper to one corner of the plate (**DOF 1Z**).

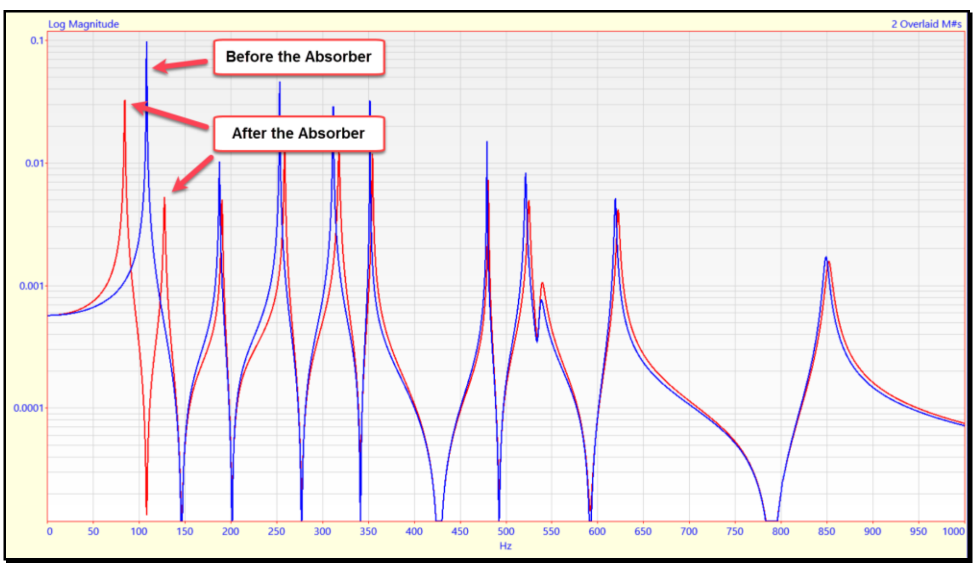

Figure 17. Synthesized FRFs (1Z:1Z) Before and After Absorber

Figure 17 shows the log magnitudes of two overlaid driving point FRFs of the plate and RIB at DOF 1Z, before (blue) and after (red) the tuned absorber was attached to the plate. These overlaid FRFs clearly show that the resonant frequency at 108 Hz has been removed from the Plate and RIB and replaced with two new resonances, one at 84 Hz and the other at 128 Hz. The two new modes also have lower Q's (less amplitude) than the Q of the mode they replaced.

The MAC values in Table 7 show that the two new mode shapes are ***essentially the same*** as the mode shape of the original 108 Hz mode. Notice also that the tuned absorber had ***very little effect*** on the other resonances of the structure.

Shape Pair	Before TA Frequency (Hz)	Before TA Damping (Hz)	After TA Frequency (Hz)	After TA Damping (Hz)	MAC
1	108.2	0.0345	84.3	0.149	0.96
2	108.2	0.0345	127.6	0.333	0.93
3	187.6	0.369	190.4	0.422	0.99
4	253.3	0.118	258.7	0.250	0.98
5	311.5	0.293	317.9	0.488	0.98
6	351.7	0.104	354.4	0.217	0.99
7	479.2	0.171	480.7	0.239	1.00
8	521.3	0.713	524.9	0.924	0.97
9	537.4	2.77	538.7	2.808	0.98
10	619.1	0.863	622.1	1.055	1.00
11	801.1	0.544	801.1	0.544	1.00

Table 7. Modes Before and After Tuned Absorber Attached at 1Z

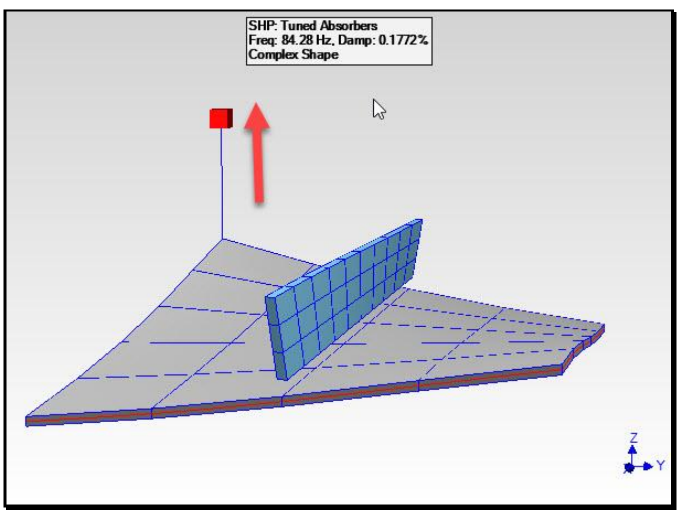

Figure 18A. Absorber In-Phase with the 84 Hz Mode

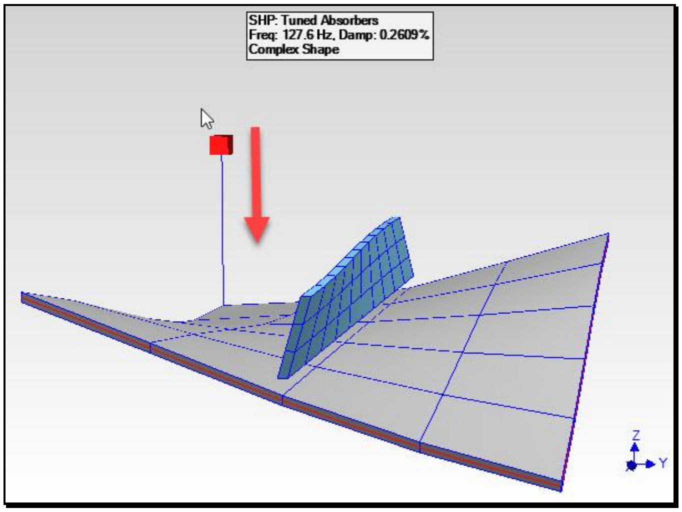

Figure 18B. Absorber Out-Of-Phase with the 128 Hz Mode

Figure 18 shows how the tuned absorber mass moves with respect to the plate. In Figure 18A the tuned absorber is ***moving in-phase*** with the plate below it. In Figure 18B it is ***moving out-of-phase*** with the plate below it. (An animated picture shows this relative motion more clearly.)

Modal Sensitivity Analysis

It is well-known that the ***modal properties*** of a structure ***are very sensitive*** to changes in its physical properties.

Because of its computational speed, SDM can be used to quickly solve for the modal parameters of ***thousands*** of potential modifications to a structure. The calculation and ordering of multiple SDM solutions from best to worst is called **Modal Sensitivity Analysis**.

EMA modes of the Plate and RIB

In a previous example, SDM was used to model the attachment of a RIB stiffener to the aluminum plate shown in Figures 5A, 5B, & 5C. To validate the SDM mode shapes using experimental data, the plate with the RIB attached was tested with a roving impact hammer test.

The plate was impacted at 24 points on the plate in the **(vertical) Z-direction** to gather enough data to uniquely define the EMA mode shapes for comparison with the SDM mode shapes. In Table 8, the first eight EMA & SDM mode shape pairs have MAC values ***close to 1.0***, indicating that they are ***closely matched.*** But the EMA & SDM modal frequencies ***are all different*** from one another.

Shape Pair	EMA Frequency (Hz)	EMA Damping (Hz)	SDM Frequency (Hz)	SDM Damping (Hz)	MAC
1	103.8	0.144	108.2	0.0345	1.00
2	188.5	0.360	187.6	0.369	0.99
3	242.5	0.262	253.3	0.118	0.99
4	259.7	0.378	311.5	0.293	0.98
5	277.4	1.164	351.7	0.104	0.97
6	468.6	0.760	479.2	0.171	0.98
7	503.6	6.035	521.3	0.713	0.97
8	572.6	4.953	537.4	2.77	0.98
9	618.8	1.828	619.1	0.863	0.87
10	657.5	6.541	801.1	0.544	0.95

Table 8. EMA versus SDM modes for the Plate with RIB

Using SDM to Explore Joint Stiffnesses

The first mode of the plate and RIB involves ***twisting of both the plate and RIB***, as shown in Figure 14. The mode shape is influenced by both the ***translational*** & ***rotational*** stiffness of the spring stiffeners used to attach the RIB to the plate.

Using the Hybrid modal model containing the mode shapes of the plate without the RIB attached, SDM can be used to quickly calculate the modes the plate and RIB using ***many different*** translational & rotational stiffnesses of the springs used to attach the RIB to the plate. These solutions are then ordered from best to worst. **Modal Sensitivity Analysis** can be performed by calculating and ordering multiple SDM solutions.

Current vs. Target Frequency

A **Modal Sensitivity** window is setup in Figure 19A to perform sensitivity calculations on the plate and RIB. The window contains two spreadsheets. The frequencies of the 30 modes of the ***unmodified*** plate and RIB substructures are listed in the **Current Frequency** column of the upper spreadsheet. This modal model contains 14 mode shapes of the plate without the RIB attached and 16 free-body mode shapes of the RIB. The mode shapes are sorted according to frequency, beginning with the rigid-body mode shapes of the RIB.

The **EMA** modal frequencies of the plate and RIB are listed in the **Target Frequency** column in the upper spreadsheet. These frequencies are used for ranking the SDM solutions from best to worst.

Ten **Shape Pairs** have been selected in the upper spreadsheet. The **Selected Pairs** are used to order the solutions from best to worst. The best solution is the one which minimizes the difference between each **Solution Frequency** and each **Target Frequency**.

Solution Space

In Table 8, the first EMA mode shape (at 103.8 Hz) has a lower frequency than the first SDM mode shape (at 108.2 Hz). Therefore, the best Modal Sensitivity solution should require ***less stiffnesses*** than the stiffnesses (**1,000,000**) used to attach the RIB to the plate.

The lower spreadsheet defines ranges of stiffness values for the translational & rotational stiffnesses of the five FEA springs. Each stiffness has a range of ***50 Steps*** (or values) in its solution space. Each SDM solution will use a stiffness value from the **Minimum Property** (**1000**) to the **Maximum Property** (**2,000,000**) of each stiffener. The solution space has 50 steps x 50 steps = ***2500 stiffness values*** in it. SDM will solve for new modes using all combinations of stiffness values in the solution space of the two stiffeners.

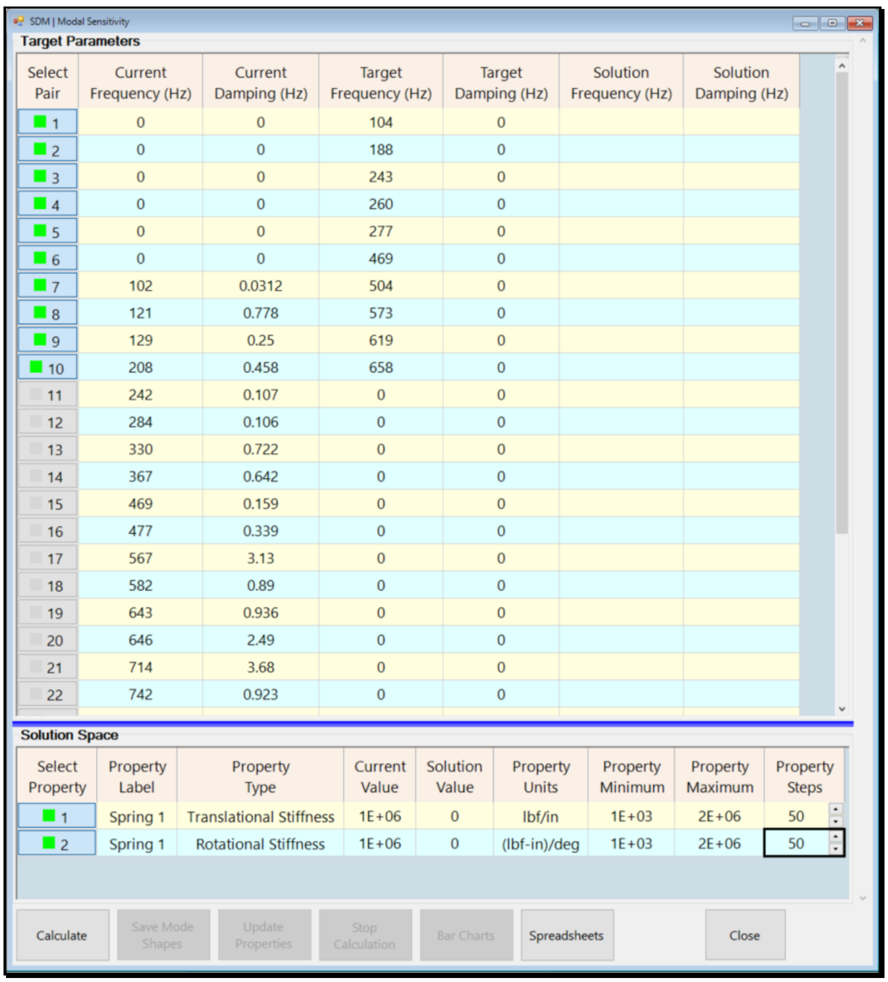

Select Pair	Current Frequency (Hz)	Current Damping (Hz)	Target Frequency (Hz)	Target Damping (Hz)	Solution Frequency (Hz)	Solution Damping (Hz)
1	0	0	104	0		
2	0	0	188	0		
3	0	0	243	0		
4	0	0	260	0		
5	0	0	277	0		
6	0	0	469	0		
7	102	0.0312	504	0		
8	121	0.778	573	0		
9	129	0.25	619	0		
10	208	0.458	658	0		
11	242	0.107	0	0		
12	284	0.106	0	0		
13	330	0.722	0	0		
14	367	0.642	0	0		
15	469	0.159	0	0		
16	477	0.339	0	0		
17	567	3.13	0	0		
18	582	0.89	0	0		
19	643	0.936	0	0		
20	646	2.49	0	0		
21	714	3.68	0	0		
22	742	0.923	0	0		

Select Property	Property Label	Property Type	Current Value	Solution Value	Property Units	Property Minimum	Property Maximum	Property Steps
1	Spring 1	Translational Stiffness	1E+06	0	lbf/in	1E+03	2E+06	50
2	Spring 1	Rotational Stiffness	1E+06	0	(lbf-in)/deg	1E+03	2E+06	50

Figure 19A. Modal Sensitivity Setup for 2500 Solutions

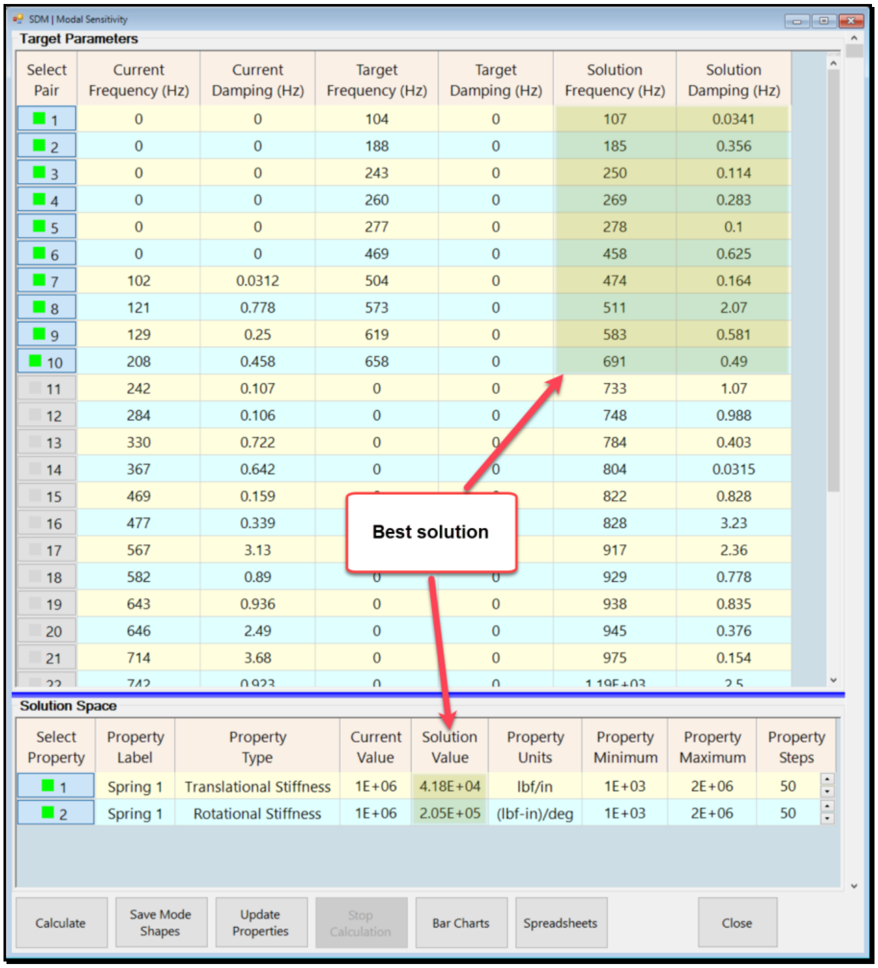

Figure 19B. Best Solution with Eight Shape Pairs Selected

Figure 19B shows the Modal Sensitivity window after 2500 solutions have been calculated and ordered from best to worst. The modal frequencies of the best solution are displayed in the **Solution Frequency** column of the upper spreadsheet. The damping values are displayed in the **Solution Damping** column.

The stiffness values used to calculate the best solution are displayed in the lower spreadsheet. The ***translational*** stiffness used to calculate the best solution is **4.18 E04 lbf/in**. The ***rotational*** stiffness used to calculate the best solution is **2.05 E05 (lbf-in)/deg**. ***Much less*** translational & rotational stiffness of the five spring stiffeners was required to ***closely match*** the frequencies of the first eight EMA modes of the plate and RIB.

FEA Modal Updating

Because of its computational speed, SDM can be used to quickly evaluate thousands of modifications to the physical properties of an FEA model. In Table 3 their MAC values indicate that each FEA mode shape of the plate ***closely matches*** with an EMA mode shape, but each FEA modal frequency ***is less than*** the EMA frequency of its matching mode shape.

The physical properties used for the plate elements in the FEA model of the aluminum plate were,

1. **Young's modulus of elasticity:** 1E07 lbf/in^2 (6.895E4 N/mm^2)
2. **Density:** 0.101 lbm/in^3 (2.796E-6 kg/mm^3)
3. **Poisson's Ratio:** 0.33.
4. **Plate thickness:** 0.375 in (9.525 mm)

The Plate is made from 6061-T651 aluminum. A more accurate handbook value for the density of this alloy of aluminum is **0.0975 lbm/in^3** (**2.966E-6 kg/mm^3**). In addition, the Quad plate elements were given a nominal thickness of **0.375 in** (**9.525 mm**). Plate stiffness is ***very sensitive*** to its thickness!

Error in the density or thickness of the elements in the FEA plate model could be the reason why the frequency of each FEA mode shape was ***less than*** the frequency of its corresponding EMA mode shape.

An **FEA Modal Updating** window is setup in Figure 20A to perform SDM calculations using multiple density and thickness values. The **FEA Frequency** of each of the 14 FEA mode shapes of the plate is listed in the upper spreadsheet. Each EMA frequency is listed as a **Target Frequency**.

All 14 mode **Shape Pairs** are selected, meaning that each **Solution Frequency** will be compared with each **Target Frequency** to order the solutions from best to worst. The best solution is the one which minimizes the difference between each **Solution Frequency** and each **Target Frequency**

The **Solution Space** is defined in the lower spreadsheet. The plate thickness and density are selected, and each has **10 Property Steps** (or values) between its **Property Minimum** & **Property Maximum**. Solutions will be calculated over a solution space of ***100 property values***, using all combinations of 10 different thicknesses and 10 different densities.

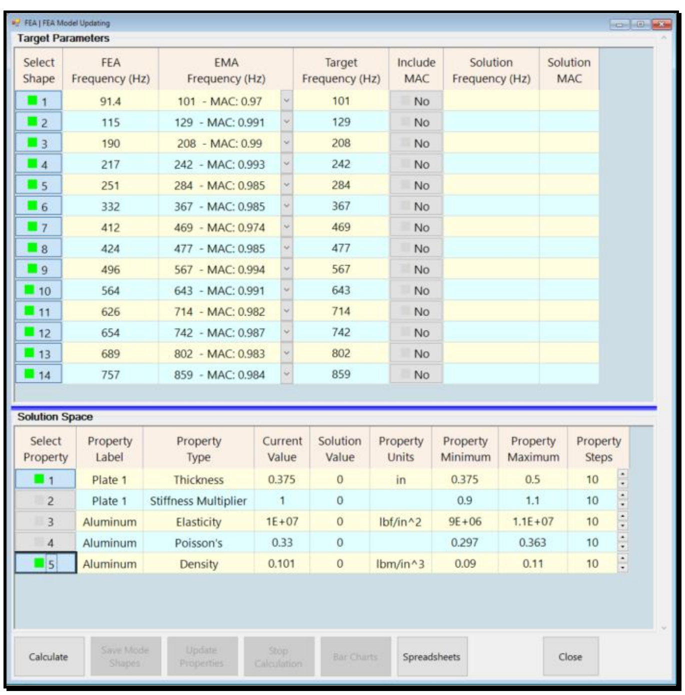
FEA | FEA Model Updating

Target Parameters

Select Shape	FEA Frequency (Hz)	EMA Frequency (Hz)	Target Frequency (Hz)	Include MAC	Solution Frequency (Hz)	Solution MAC
1	91.4	101 - MAC: 0.97	101	No		
2	115	129 - MAC: 0.991	129	No		
3	190	208 - MAC: 0.99	208	No		
4	217	242 - MAC: 0.993	242	No		
5	251	284 - MAC: 0.985	284	No		
6	332	367 - MAC: 0.985	367	No		
7	412	469 - MAC: 0.974	469	No		
8	424	477 - MAC: 0.985	477	No		
9	496	567 - MAC: 0.994	567	No		
10	564	643 - MAC: 0.991	643	No		
11	626	714 - MAC: 0.982	714	No		
12	654	742 - MAC: 0.987	742	No		
13	689	802 - MAC: 0.983	802	No		
14	757	859 - MAC: 0.984	859	No		

Solution Space

Select Property	Property Label	Property Type	Current Value	Solution Value	Property Units	Property Minimum	Property Maximum	Property Steps
1	Plate 1	Thickness	0.375	0	in	0.375	0.5	10
2	Plate 1	Stiffness Multiplier	1	0		0.9	1.1	10
3	Aluminum	Elasticity	1E+07	0	lbf/in^2	9E+06	1.1E+07	10
4	Aluminum	Poisson's	0.33	0		0.297	0.363	10
5	Aluminum	Density	0.101	0	lbm/in^3	0.09	0.11	10

Calculate | Save Mode Shapes | Update Properties | Stop Calculation | Bar Charts | Spreadsheets | Close

Figure 20A. Setup for 100 FEA Model Updating Solutions

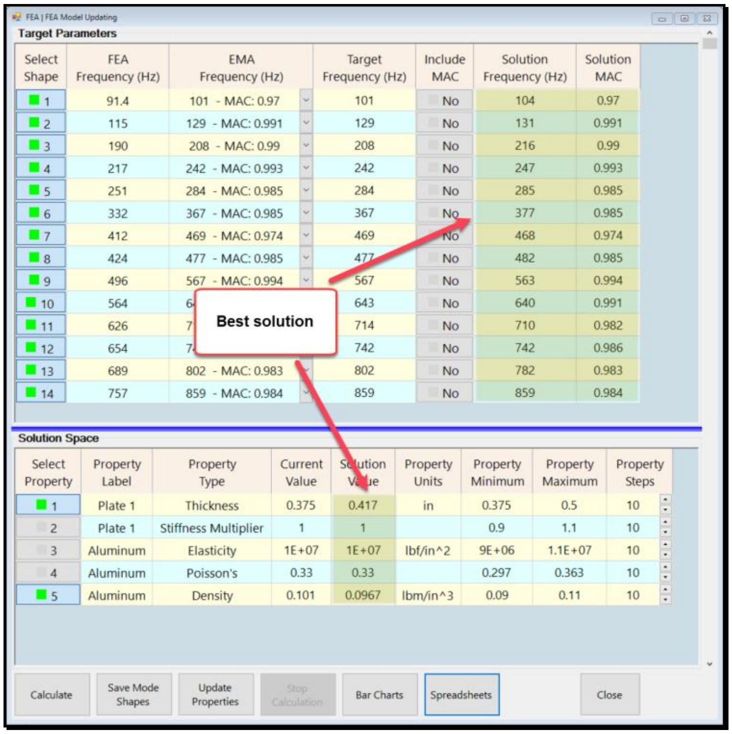

Select Shape	FEA Frequency (Hz)	EMA Frequency (Hz)	Target Frequency (Hz)	Include MAC	Solution Frequency (Hz)	Solution MAC
1	91.4	101 - MAC: 0.97	101	No	104	0.97
2	115	129 - MAC: 0.991	129	No	131	0.991
3	190	208 - MAC: 0.99	208	No	216	0.99
4	217	242 - MAC: 0.993	242	No	247	0.993
5	251	284 - MAC: 0.985	284	No	285	0.985
6	332	367 - MAC: 0.985	367	No	377	0.985
7	412	469 - MAC: 0.974	469	No	468	0.974
8	424	477 - MAC: 0.985	477	No	482	0.985
9	496	567 - MAC: 0.994	567	No	563	0.994
10	564	[illegible]	643	No	640	0.991
11	626	[illegible]	714	No	710	0.982
12	654	[illegible]	742	No	742	0.986
13	689	802 - MAC: 0.983	802	No	782	0.983
14	757	859 - MAC: 0.984	859	No	859	0.984

Select Property	Property Label	Property Type	Current Value	Solution Value	Property Units	Property Minimum	Property Maximum	Property Steps
1	Plate 1	Thickness	0.375	0.417	in	0.375	0.5	10
2	Plate 1	Stiffness Multiplier	1	1		0.9	1.1	10
3	Aluminum	Elasticity	1E+07	1E+07	lbf/in^2	9E+06	1.1E+07	10
4	Aluminum	Poisson's	0.33	0.33		0.297	0.363	10
5	Aluminum	Density	0.101	0.0967	lbm/in^3	0.09	0.11	10

Figure 20B. Best Solution for Updating Density & Thickness

The properties of the ***original*** FEA model are required in order to update those properties.

To perform FEA Model Updating, the properties of the ***unmodified*** model must be removed from the mass & stiffness matrices before the new properties can be added.

Figure 20B shows the Model Updating window after 100 solutions have been calculated and ordered from best to worst. For all 14 Shape Pairs, each **Solution Frequency** ***closely matches*** each **Target Frequency**. The **Solution MAC** between each **Shape Pair** also indicates that the mode shapes of all 14 mode shapes were not changed by updating the density & thickness.

The updated density (**0.0967**) more closely matches the handbook density for 6061-T651 aluminum. The updated thickness (**0.417 in.**) is more than the thickness originally used but it resulted in new modal frequencies that ***more closely matched*** the experimental frequencies.

Difference Between Modal Sensitivity and FEA Model Updating

In order to calculate the new modes of a modified structure, SDM only requires a **modal model** of the ***unmodified*** structure together with FEA elements. For Modal Sensitivity Analysis the properties of modification elements are used. For FEA Modal Updating the properties of FEA elements of the FEA model are used.

In **Modal Sensitivity Analysis**, multiple SDM solutions are calculated over a solution space of modification element properties, and the solutions are ordered from best to worst based on how closely the Solution frequency & damping of each selected Shape Pair match the Target modal frequency & damping.

In **FEA Model Updating**, multiple SDM solutions are calculated over a solution space of FEA model properties, and the solutions are ordered from best to worst based on how closely the Solution frequency & mode shape of each selected Shape Pair match the Target modal frequency & mode shape.

Whether SDM is used for Modal Sensitivity or FEA Model Updating studies, ***thousands of potential property changes*** can be quickly evaluated and sorted from best to worst based on how close a Solution is to Target values. In these applications, SDM is very useful for ***"closing the gap"*** between analytical and experimental results.

REFERENCES

1. Hallquist, J. "Modification and Synthesis of Large Dynamic Structural Systems" Ph.D. Dissertation, Michigan Technological University, 1974.
2. Formenti, D. & Welaratna, S. "Structural Dynamics Modification - An Extension to Modal Analysis" SAE Paper No. 811043, Oct. 1980.
3. Structural Measurement Systems, Inc. "An Introduction to the Structural Dynamics Modification System", Technical Note No.1, February 1980.
4. Ramsey, K. & Firmin, A. "Experimental Modal Analysis Structural Modifications and FEM Analysis - Combining Forces on a Desktop Computer" First IMAC Proceedings, Orlando, Florida, Nov. 8-10, 1982
5. Wallack, P., Skoog, P., and Richardson, M.H. "Simultaneous Structural Dynamics Modification S^2DM)" Proc. of 6^{th} IMAC, Kissimmee, FL, 1988
6. Bathe, K.J., and Wilson, E.L. "Numerical Methods in Finite Element Analysis" Prentice Hall, Inc., 1976.
7. Yang, T.Y. "Finite Element Structural Analysis" Prentice Hall, Inc., 1986.
8. McGuire, W., and Gallagher, R.H. "Matrix Structural Analysis" John Wiley & Sons, 1979.